# Supramolecular Networks Derived from Hexacyanoferrates and Nitrogen Heterocyclic Cations[§]

*Pantelis Xydias,[a] Smaragda Lymperopoulou,[b] Vasiliki Dokorou, Manolis Manos, John C. Plakatouras**

Department of Chemistry, University of Ioannina, 451 10, Greece

Present Addresses: [a]School of Chemistry, University of Glasgow, Joseph Black Building. University Avenue, Glasgow, G12 8QQ, Scotland; [b]School of Chemistry, University of Southampton, Highfield Campus, Southampton SO17 1BJ, UK

[§] Dedicated to Professor Spyros P. Perlepes on the occasion of his 65th birthday.

* Corresponding author: iplakatu@cc.uoi.gr, phone: +30-2651-008417;

fax: +30-2651-008786

**Abstract**

Eight novel supramolecular framworks $(bpyH_2)_2[Fe(CN)_6]\cdot 2H_2O$ (**1**), $(bpyH_2)(H_3O)[Fe(CN)_6]$ (**2**), $(bpeH_2)(H_3O)[Fe(CN)_5(CNH)]\cdot H_2O$ (**3**), $(bpeH_2)(H_5O_2)[Fe(CN)_6]\cdot 2H_2O$ (**4**), $(dabcoH_2)(H_3O)[Fe(CN)_6]\cdot 2H_2O$ (**5**), $(ampyH_2)_2[Fe(CN)_6]\cdot 2H_2O$ (**6**), $(tptzH_3)_2[Fe(CN)_4(CNH)_2]_3\cdot 10H_2O$ (**7**), and $(tptzH_3)[Fe(CN)_6]\cdot 3H_2O$ (**8**) (where bpy =4,4'-bipyridine, bpe = 1,2-bis(4-pyridyl)ethylene, dabco = 1,4-diazabicyclo[2.2.2]octane, ampy = 4-aminomethylpyridine, tptz = tris(4-pyridyl)triazine) have been synthesized by the reaction of the nitrogen heterocycle with ferrocyanide or ferricyanide salts, under mild conditions. The supramolecular structures are constructed mainly by cooperative hydrogen bonding between the inorganic anions, the organic cations and oxoniums or lattice water molecules. There are some characteristic features that can separate the compounds in groups. Those are a) increase of H-bonding ability by formation of supramolecular complexes, b) formation of hydro- and dihydro-hexacyanoferrates and c) the participation of the cationic heterocycle as constituent of the structure or as a guest. The structures are additionally discussed in terms of topology.

Keywords: supramolecular networks; cyanometallates; hexacyanoferrates; nitrogen heterocycles; organic cations; crystal engineering; topology

## 1. Introduction

The construction of discrete supramolecules or extended networks through non-covalent interactions is a continuing challenge in crystal engineering. Since the molecular and crystal structures determine the properties of the solids and in turn those structures are determined to certain extend by interactions other than covalent and coordination bonds, the necessity of the study of those interactions becomes obvious. [1,2]

Of the weak interactions, hydrogen bonds are the most directional and they have been exploited extensively by researchers working on the field of crystal engineering. Modular synthetic strategies where anions (usually metal complexes) with hydrogen bond acceptor capability are crystallized as salts of cations (mostly organic) with hydrogen bond donor capability have been used by various research groups.[3] Similar approaches have been utilized for organic systems as well using organic or organometallic anions.[4] Intermolecular interactions such as H-bonds N-H···anion serve as supramolecular synthons [5] and control the packing of molecular tectons [6] into the periodic motifs that form the basis of their crystal structures.

On the other hand, the interest on cyanometalate compounds is dated back to the 19th century, and they have used for studies in electron transfer processes [7], for their interesting magnetic [8] and optical properties. [9] They are also appealing members in the field of crystal engineering [3d, 10], with applications such as thermal switches [11], soft crystalline materials [12] and materials with selective absorption properties.[13].

Cyanometalate compounds usually crystallize with a number of solvent molecules which, in turn, may form hydrogen bonds either with the coordinated cyanides or the cations. For compounds containing hexacyanometalates as anions, the number of hydrogen bonding interactions and the probability of interesting topologies is enhanced.

The use of the network or topological approach to crystal chemistry has proved to be in the case of crystal engineering a useful analysis tool for the structures through simplification of the complicated supramolecular architectures to schematized nets. However, as already observed,[14] the topological rationalization of hydrogen-bonded frameworks is more difficult than that of MOFs because the nodes and linkers are usually more ambiguous to select [for example several times we have encountered H-bonds of various strengths].

Strong non-covalent interactions, mainly H-bonding, are prerequisite for the stability of a functional supramolecular network. Therefore, the choice of molecular building blocks whose structure and functions may be tuned by using appropriate strategies with the help of crystal engineering is critical. Bearing this in mind, we have chosen $[Fe(CN)_6]^{n-}$ (n = 3, 4) as acceptors and protonated pyridine containing organic molecules as donors for scanning the supramolecular architectures would be formed and to possibly find the factors govern the resulting formulations. Herein we report the synthesis and structural characterization of the new networks derived by cyanoferrates(II) or (III) and 4,4'-dipyridinium ($bpyH_2^{2+}$), 1,2-di(4-pyridinium)ethene ($bpyeH_2^{2+}$), diazabicyclooctanium ($dabcoH_2^{2+}$), 4-ammoniummethyl-pyridinium ($ampyH_2^{2+}$) and tris(4-pyridinium)triazine ($tptzH_3^{3+}$). A survey of the published literature (CSD) reveals that there are previous studies with $bpeH_2^{2+}$ [12] or singly protonated bipyridine ($bpyH^+$) [13] and cyanoferrates while metallocyanates of $dabcoH_2^{2+}$, $ampyH_2^{2+}$ and $tptzH_3^{3+}$ are totally absent.[15]

## 2. Experimental

### 2.1 Materials and Measurements

All reagents and solvents were of commercially available reagent quality unless otherwise stated. tris(4-pyridyl)triazine (tptz) was prepared by fusion of an equimolar mixture of 4-cyanopyridine and KOH and subsequent recrystallization of the resulting solid from boiling pyridine. All the reactions for the preparation of the hexacyanometallate salts were performed at room temperature and no special conditions were demanded. C, H, and N analyses were conducted by the University of Ioannina, Greece, Microanalytical Service. IR spectra were recorded on a Perkin–Elmer Spectrum GX FT-IR spectrophotometer with samples as KBr pellets. UV–Vis spectra on solid state (Diffuse Reflectance Spectra) were recorded on a Shimadzu UVPC 2401 spectrophotometer; the samples were prepared as 1:2 solid mixtures in $BaSO_4$, which was also used as reference. TG-DTA analysis was carried out under synthetic air, at a scan speed of 5 $^oC$/min, on a Shimadzu DTG 60 apparatus with the sample size being *ca.* 5 mg. X-ray powder diffraction patterns were recorded on a Siemens (now Bruker) D8 ADVANCE diffractometer.

### 2.2 Syntheses

*2.2.1 $(bpyH_2)_2[Fe(CN)_6]\cdot 2H_2O$ (**1**)*

$Na_4[Fe(CN)_6]\cdot 10H_2O$ (0.250 g, 0.5 mmol) was dissolved in 10 mL of a 1:2 solvent mixture of DMF/$H_2O$ and to this a warm solution of bpy (0.080 g, 0.5 mmol) in $H_2O$ (15 mL) was added. To the resulting solution 0.5 mL 1 M HCl were added and it was placed in the fridge at 4 $^oC$. Dark crystals formed after 1 day. Yield: 38 % based on Fe. Anal. Calc. for $C_{26}H_{24}FeN_{10}O_2$ (fw = 564.38): C, 55.33; H, 4.29; N, 24.82. Found: C, 54.78; H, 4.35; N, 24.57 %. IR (KBr, $cm^{-1}$): 3440 m, 3431 m, 3119 mw, 2650 b, 2042 s, 1620 s, 1480 m, 1008 m, 812w.

*2.2.2 ($bpyH_2$)($H_3O$)[$Fe(CN)_6$] (**2**)*

A solution of $K_3[Fe(CN)_6]\cdot 3H_2O$ (0,304 g, 0.79 mmol) in 5 mL of 2 M HCl was added to a solution of bpy (0.144 g, 0.92 mmol ) in 5 mL of the same solvent. Yellow crystals were precipitated after 1 day at 4 $^oC$. Yield 68 % based on Fe. Anal. Calc. for $C_{16}H_{13}FeN_8O$ (fw = 389.17): C, 49.38; H, 3.37; N, 28.79. Found: C, 49.01; H, 3.60; N, 28.11 %. IR (KBr, $cm^{-1}$): 3427 m, 3390 mb, 3097 mw, 2575 mb, 2040 s, 1610 s, 1480 m, 999 m, 805w.

*2.2.3 ($bpeH_2$)($H_3O$)[$Fe(CN)_5(CNH)$]·$H_2O$ (**3**)*

A solution of $Na_4[Fe(CN)_6]\cdot 10H_2O$ (0.084 g, 0.2 mmol) in 5mL HCl 1M was added to a solution of bpe (0.037 g, 0.2 mmol) in 5 mL of the same solvent. Nice red crystals separated from the mother liquid after several hours in the fridge. Yield 67 % based on Fe. Anal. Calc. for $C_{18}H_{18}FeN_8O_2$ (fw = 434.23): C, 49.79; H, 4.18; N, 25.81. Found: C, 49.03; H, 4.32; N, 26.01 %. IR (KBr, $cm^{-1}$): 3430mb, 3043 w, 2610 b, 2047 s, 2035 sh, 1625 s, 1613 msh, 1501 m, 778 m, 540 w.

*2.2.4 ($bpeH_2$)($H_5O_2$)[$Fe(CN)_6$]·$2H_2O$ (**4**)*

Compound **4** crystallized as yellow solid from a solution containing $K_3[Fe(CN)_6]\cdot 3H_2O$ (0.047 g, 0.142 mmol) and bpe (0.021 g, 0.120 mmol) in 7 mL $H_2O$ and 2 mL concentrated commercial HCl solution after two days in the fridge. Yield: 41 % based on bpe. Anal. Calc. for $C_{18}H_{22}FeN_8O_4$ (fw = 470.26): C, 45.97; H, 4.72; N, 23.83. Found: C, 46.03; H, 4.93; N, 23.54 %. IR (KBr, $cm^{-1}$): 3426mb, 3040 w, 2590 b, 2043 s, 1624 s, 1617 msh, 1500 m, 781 m, 539 w.

*2.2.5 ($dabcoH_2$)($H_3O$)[$Fe(CN)_6$]·$2H_2O$ (**5**)*

Compound **5** crystallized as yellow solid from a solution containing $K_3[Fe(CN)_6]\cdot 3H_2O$ (0.306 g, 0.80 mmol) and dabco (0.090 g, 0.80 mmol) in 20 mL 1 M HCl after several hours in the fridge at 4 $^oC$. Yield: 66 % based on Fe. Anal. Calc. for $C_{12}H_{21}FeN_8O_3$ (fw = 381.19): C, 37.81; H,

5.55; N, 29.40. Found: C, 38.00; H, 5.57; N, 29.49 %. IR (KBr, $cm^{-1}$): 3442 mb, 2955 mw, 2920 w, 2760 b, 2535 mb, 2039 s, 1450 s, 1428 s, 1375 m, 1050 vs, 840 s.

*2.2.6 $(ampyH_2)_2[Fe(CN)_6]\cdot 2H_2O$ (**6**)*

A solution of $Na_4[Fe(CN)_6]\cdot 10H_2O$ (0.250 g, 0.5 mmol) in 15 mL of a 1:2 DMF/$H_2O$ solvent mixture plus 400 µL of HCl 1M was added to 15 mL of an aqueous solution containing 100 µL (1.0 mmol) ampy and 400 µL HCl 1 M. Yellow crystals precipitated after few hours in the fridge. Yield: 39%. Anal. Calc. for $C_{18}H_{24}FeN_{10}O_2$ (fw = 468.29): C, 46.17; H, 5.17; N, 29.91. Found: C, 46.10; H, 5.27; N, 29.39 %. IR (KBr, $cm^{-1}$): 3471 mb, 3070w, 2920 w, 2763 b, 2042 s, 1601 s, 1405 m, 778 m.

*2.2.7 $(tptzH_3)_2[Fe(CN)_4(CNH)_2]_3\cdot 10H_2O$ (**7**)*

In a solution containing 5 mL DMF, 1 mL DMSO, 0.5 mL concentrated HCl, and 0.150 g (0.48 mmol) tptz added an aqueous solution (8 mL) of $Na_4[Fe(CN)_6]\cdot 10H_2O$ (0.233 g, 0.48 mmol) and the resulting blue solution was placed uncovered in a desiccator containing anhydrous $CaCl_2$. Blue crystals were formed after five days. Yield: 32 %. %. Anal. Calc. for $C_{54}H_{56}Fe_3N_{30}O_{10}$ (fw = 1452.75): C, 44.64; H, 3.89; N, 28.92. Found: C, 44.12; H, 4.00; N, 28.61 %. IR (KBr, $cm^{-1}$): 3462 mb, 3051 w, 2662 b, 2057 s, 2042 s, 1526 s, 1469 mw, 1434 w, 1373 s, 1000 m, 760 s.

*2.2.8 $(tptzH_3)[Fe(CN)_6]\cdot 3H_2O$ (**8**)*

Compound **8** was prepared with the same manner as **7**, using $K_3[Fe(CN)_6]\cdot 3H_2O$ (0.184 g, 0.48 mmol) as the anion source. Dark yellowish orange crystals was formed after 3 days in the desiccator. Yield: 39 %. Anal. Calc. for $C_{24}H_{21}FeN_{12}O_3$ (fw = 581.35): C, 49.58; H, 3.64; N, 28.91. Found: C, 49.02; H, 3.78; N, 28.36 %. IR (KBr, $cm^{-1}$): 3435 mb, 3049 w, 2572 b, 2048 s, 1528 s, 1466 mw, 1436 w, 1369 s, 1001 m, 762 s.

**2.3 Crystal Structure Determinations**

Compounds **1**, **4**, **6**, **7**, **8**: Suitable crystals were glued to a thin glass fibre with cyanoacrylate (super glue) adhesive. X-ray diffraction intensities were collected at room temperature on a Siemens (now Bruker) P4 diffractometer employing graphite monochromated Mo Ka radiation, λ = 0.71073 Å. Compounds **2**, **3**, **5**: Data were collected on an Oxford Diffraction diffractometer, equipped with a CCD area detector and a graphite monochromator utilizing Mo Ka radiation (λ = 0.71073 Å). Suitable crystals were attached to glass fibers using paratone-N oil and transferred to a goniostat where they were cooled for data collection.

The structures were solved by direct methods (SIR-2014) [16] and refined by full-matrix least squares techniques on $F^2$ (SHELXL 2016/6) [17] via ShelXle interface. [18] The handling of compound **3** was not without problems. Attempts to solve and refine it with different space groups (i.e. C2/c, Cc, and I2/a) were met several non-positive definite atoms. The best results were obtained using the non-standard space group Ia and racemic twinning which lead to a BASF value of 0.34. All non-hydrogen atoms were refined anisotropically. Some of the organic H atoms were located by difference Fourier maps, but finally all of them were introduced in idealized positions and treated as riding on the parent non-hydrogen atoms. The N-H protons were located and refined with SHELX restraints. Some of the water protons were located by difference Fourier maps while the rest were calculated with CALCOH [19]. All of them were refined isotropically utilizing SHELX restrains. Simulated XRPD patterns were produced with PLATON [14]. The topological study was performed with the ToposPro software package. [20] Table 1 contains crystal data and details of refinement for **1** – **8** and Table 2 contains the structural characteristics of the H-bonds discussed in the text, Separately, crystal data and details of refinement for **1** – **8** in addition to selected bond

distances and angles are presented in Tables S1 – S16. Full details on the structures can be found in the CIF files in the ESI.

**Table 1** Crystal data and details of the structure determination for the prepared compounds.

| Compound | **1** | **2** | **3** | **4** | **5** | **6** | **7** | **8** |
|---|---|---|---|---|---|---|---|---|
| Formula | $C_{26}H_{24}N_{10}O_2Fe$ | $C_{16}H_{13}N_8OFe$ | $C_{18}H_{18}N_8O_2Fe$ | $C_{18}H_{21}N_8O_4Fe$ | $C_{18}H_{21}N_8O_4Fe$ | $C_{18}H_{24}N_{10}O_2Fe$ | $C_{27}H_{28}N_{15}O_5Fe_{1.5}$ | $C_{24}H_{21}N_{12}O_3Fe$ |
| Formula Weight | 564.39 | 389.19 | 434.25 | 468.78 | 381.22 | 468.32 | 726.42 | 581.38 |
| Crystal System | monoclinic | monoclinic | monoclinic | monoclinic | triclinic | triclinic | monoclinic | monoclinic |
| Space group | C2/m | $P2_1$ | Ia | C2/c | P-1 | P-1 | C2/c | C2/c |
| *a*, (Å) | 13.927(2) | 7.269(4) | 16.2606(6) | 10.745(1) | 8.0888(2) | 7.838(5) | 24.873(5) | 13.151(5) |
| *b*, (Å) | 9.064(1) | 14.245(5) | 10.0711(2) | 12.657(1) | 14.5001(3) | 8.837(5) | 14.270(4) | 12.193(5) |
| *c*, (Å) | 10.161(1) | 8.750(4) | 14.5502(5) | 17.043(1) | 14.9025(2) | 8.922(5) | 20.137(5) | 17.580(6) |
| *α*, (°) | 90 | 90 | 90 | 90 | 90.153(1) | 63.590(5) | 90 | 90 |
| *β*, (°) | 95.72(1) | 99.005(5) | 122.818(5) | 103.31(1) | 90.128(2) | 73.340(5) | 110.20(1) | 108.19(1) |
| *γ*, (°) | 90 | 90 | 90 | 90 | 98.475(2) | 88.980(5) | 90 | 90 |
| V, ($Å^3$) | 1276.3(3) | 894.9(7) | 2002.47(16) | 2255.6(3) | 1728.79(6) | 525.9(5) | 6708(3) | 2678.1(18) |
| Z | 2 | 2 | 4 | 2 | 2 | 1 | 4 | 4 |
| D(calc) ($g/cm^3$) | 1.469 | 1.444 | 1.440 | 1.380 | 1.465 | 1.479 | 1.439 | 1.442 |
| μ(MoKa) ($mm^{-1}$) | 0.637 | 0.865 | 0.785 | 0.709 | 0.901 | 0.755 | 0.718 | 0.614 |

| | | | | | | | | |
|---|---|---|---|---|---|---|---|---|
| F(000) | 584 | 398 | 896 | 970 | 796 | 244 | 2992 | 1196 |
| Crystal Size (mm) | 0.05x0.10x0.20 | 0.12x0.17x0.20 | 0.09x0.11x0.21 | 0.08x0.12x0.21 | 0.08x0.09x0.31 | 0.10x0.12x0.24 | 0.08x0.12x0.21 | 0.10x0.12x0.24 |
| Temperature (K) | 293 | 100 | 100 | 293 | 100 | 293 | 293 | 293 |
| $\lambda$, (Å) | 0.71073 | 0.71073 | 0.71073 | 0.71073 | 0.71073 | 0.71073 | 0.71073 | 0.71073 |
| $\vartheta$ range ($^{o}$) | 2.0 – 25.0 | 3.2 – 30.3 | 3.3 – 30.3 | 2.5 – 25.0 | 3.5 – 30.3 | 2.6 – 24.4 | 2.1 – 25.0 | 2.3, 25.0 |
| h | -1 – 16 | -10 – 6 | -21 – 15 | -1 – 12 | -10 – 11 | -1 – 9 | -1 – 29 | -1: 15 |
| k range | 0 – 10 | -19 – 20 | -13 – 13 | 0 – 15 | -20 – 15 | -9 – 9 | 0 – 16 | 0: 14 |
| l | -12 – 12 | -12 – 11 | -15 – 20 | -20 – 19 | -20 – 20 | -10 – 10 | -23 – 22 | -20: 20 |
| Tot., Uniq. Data, | 1334, 1194 | 8148, 4663 | 7641, 3280 | 2311, 1972 | 15622, 8993 | 2086, 1679 | 6288, 5861 | 2667, 2334 |
| R(int) | 0.102 | 0.032 | 0.018 | 0.019 | 0.028 | 0.061 | 0.049 | 0.050 |
| Observed Data | 1003, [I>2.0σ(I)] | 4006, [I>2.0σ(I)] | 3160, [I>2.0σ(I)] | 1579, [I>2.0σ(I)] | 7302, [I>2.0σ(I)] | 1284, [I>2.0σ(I)] | 4218, [I>2.0σ(I)] | 2032, [I>2.0σ(I)] |
| Nref, Npar | 1194, 118 | 4663, 254 | 3280, 305 | 1972, 176 | 8993, 506 | 1679, 166 | 5861, 503 | 2334, 204 |
| R, wR2 | 0.0443, 0.1212 | 0.0354, 0.0708 | 0.0378, 0.0952 | 0.0379, 0.1041 | 0.0341, 0.0778 | 0.0691, 0.1886 | 0.0531, 0.1511 | 0.0586, 0.1891 |
| GoF | 1.14 | 0.94 | 1.03 | 1.04 | 1.02 | 1.05 | 1.00 | 1.08 |
| Max. and Av. Shift/Error | 0.00, 0.00 | 0.00, 0.00 | 0.04, 0.00 | 0.00, 0.00 | 0.00, 0.00 | 0.00, 0.00 | 0.00, 0.00 | 0.00, 0.00 |

| | | | | | | | | |
|---|---|---|---|---|---|---|---|---|
| Min. and Max. Resd. Dens. [e/Å$^3$] | -0.57, 0.36 | -0.31, 0.47 | -0.53, 1.69 | -0.24, 0.49 | -0.47, 0.47 | -1.33, 0.94 | -0.66, 0.44 | -0.68, 1.08 |

## 3. Results and Discussion

### 3.1 Synthetic Comments and Properties

The compounds presented here have been synthesized using simple routes and mild conditions. There are though a couple of interesting synthetic points that are worthy to be mentioned.

For all the isolation of all compounds the products were removed from the parental mixture as soon as possible after their formation, and this is probably the reason for the relatively low preparative yiels. Prolonged crystallization procedures lead to mixtures, as shown by the comparison of their X-ray powder diffraction patterns with those simulated from the single crystal data.

Most of the synthetic reactions were performed in aqueous media. Compounds **7** and **8** were isolated from a mixture of polar organic solvents due to the insolubility of tptz. Despite the presence of solvents other than water in the synthetic procedure of **7** and **8** (DMF, DMSO) and **1** and **6** (DMF) none of the products contained those solvents in the crystal lattice. This is probably due to the possibility of blocking H-bonding donor sites and reducing the stability or preventing the formation of an H-bonded network.

The compounds in general are stable at room temperature for extended periods. As far as their thermal stability is concerned, as studied with TG/DTA measurements under synthetic air flow, they can be separated in three distinct categories, depending on their structures discussed bellow. (a) Those containing only H-bonded water molecules (compounds **1**, **6**, **7**, **8**), (b) compound **2** that contains only hydronium ions, and (c) those containing both water molecules and hydronium cations (compounds **3**, **4**, **5**).

Group (a) compounds are stable up to 90 $^{o}$C, where a weight loss begins and continues up to *ca*. 115 $^{o}$C. The procedure is endothermal as shown by the DTA curve and leads to a plateau.

Compound **2** is the most thermally stable of all compounds presented here. The first curve inflection in the TG graph begins at 139 $^{o}$C and is accompanied by an endotherm peak in the DTA curve. A plateau is reached at 165 $^{o}$C and the mass loss corresponds very well to the water content of 2 (Found: 4.5, Calcd: 4.63 %).

The water loss of compounds belonging to group © is more complicated, and it appears to be a combination of the previously described procedures. They begin to lose their water content just above 85 $^{o}$C and a plateau is reached at approximately 140 $^{o}$C.

The decomposition of the thermal intermediates, obtained after the water content is removed, is complicated as shown by the plurality of the curve inflections in the TG graph and the number of the exotherm peaks in the DTA graph, which exceeds 2. Those decompositions begin above 250 and are completed at 450 $^{o}$C. The most stable intermediates are those of compounds 7 and 8, probably due to the extended aromatic ring systems of the cations. The final residue in all cases looks carbonaceous and has been assigned to $Fe_2O_3$ from weight loss calculations.

Diffuse reflectance electronic spectra for compounds **1**, **3**, **6**, and **7** show the characteristic broad band of the so-called outer sphere charge transfer between 500 and 600 nm.

**Table 2**. Conventional H–bonding interactions for the prepared compounds.

| D – H ··· A | D – H (Å) | H ··· A (Å) | D ··· A (Å) | ∠ DHA (º) | Symmetry |
|---|---|---|---|---|---|
| *$(bpyH_2)_2[Fe(CN)_6]\cdot 2H_2O$ (**1**)* | | | | | |
| O(2) – H(1W) ··· N(1) | 0.93(10) | 1.94(10) | 2.875(7) | 177(8) | -x, y, -z-1 |
| O(2) – H(2W) ··· N(1) | 0.76(9) | 2.28(9) | 3.028(7) | 169(8) | |
| N(4) – H(4N) ··· N(3) | 0.92(6) | 2.13(4) | 2.858(5) | 135.0(13) | x, y, z-1 |
| *$(bpyH_2)(H_3O)[Fe(CN)_6]$ (**2**)* | | | | | |
| O(1) – H(1W) ··· N(6) | 0.90(4) | 1.76(4) | 2.652(4) | 173(4) | -x+1, y+1/2, -z+1 |
| O(1) – H(2W) ··· N(2) | 0.95(5) | 1.70(5) | 2.642(4) | 173(5) | -x+1, y+1/2, -z |
| O(1) – H(3W) ··· N(3) | 1.09(7) | 1.42(7) | 2.509(4) | 179(8) | |
| N(7) – H(7N) ··· N(5) | 0.88(3) | 1.87(3) | 2.752(4) | 178(3) | -x+2, y+1/2, -z |
| N(8) – H(8N) ··· O(1) | 0.84(3) | 2.45(4) | 2.945(4) | 118(3) | -x, y-1/2, -z |
| N(8) – H(8N) ··· N(4) | 0.84(3) | 2.51(4) | 3.153(5) | 134(4) | -x+1, y-1/2, -z |
| *$(bpeH_2)(H_3O)[Fe(CN)_5(CNH)]\cdot H_2O$ (**3**)* | | | | | |
| N(4) – H(1W) ··· O(1B) | 0.88(10) | 1.66(10) | 2.512(15) | 163(8) | |
| N(4) – H(1W) ··· O(1A) | 0.88(10) | 1.66(11) | 2.474(17) | 153(9) | |
| O(1B) – H(2W) ··· N(6) | 0.87(7) | 1.96(7) | 2.740(15) | 149(7) | x+1/2, y-1/2, z+1/2 |
| O(1B) – H(3W) ··· N(3) | 0.80(9) | 1.87(8) | 2.587(15) | 149(6) | x+1/2, -y+2, z |
| O(2) – H(4W) ··· N(6) | 0.85(7) | 1.99(8) | 2.795(6) | 158(6) | |
| O(2) – H(5W) ··· N(1) | 0.88(5) | 1.86(5) | 2.736(4) | 178(8) | x, -y+3/2, z-1/2 |
| O(2) – H(6W) ··· N(2) | 0.98(13) | 1.61(13) | 2.517(6) | 152(8) | x+1/2, -y+2, z |
| N(7) – H(7N) ··· N(5) | 0.85(5) | 1.96(5) | 2.744(6) | 154(6) | x-1/2, -y+1, z |
| N(8) – H(8N) ··· N(1) | 0.86(5) | 2.12(5) | 2.899(8) | 150(5) | x+1/2, -y+1, z |
| *$(bpeH_2)(H_5O_2)[Fe(CN)_6]\cdot 2H_2O$ (**4**)* | | | | | |
| O(1) – H(1W) ··· N(2) | 0.84(5) | 2.36(5) | 2.685(4) | 104(4) | |

| | | | | | |
|---|---|---|---|---|---|
| O(1) – H(2W) ··· O(2B) | 0.91(5) | 1.72(6) | 2.57(2) | 156(5) | -x, -y+1, -z |
| O(1) – H(2W) ··· O(2A) | 0.91(5) | 1.72(7) | 2.60(4) | 163(5) | -x, -y+1, -z |
| O(1) – H(3W) ··· O(1) | 1.228(4) | 1.228(4) | 2.456(3) | 179(7) | -x+1, y, -z+1/2 |
| N(4) – H(4N) ··· N(3) | 0.8600 | 2.0000 | 2.803(3) | 155.00 | x+1/2, y-1/2, z |
| O(2B) – H(5B) ··· N(1) | 0.78(9) | 2.44(9) | 3.20(2) | 165(10) | -x, y, -z-1/2 |
| *(dabcoH$_2$)(H$_3$O)[Fe(CN)$_6$]·2H$_2$O (**5**)* | | | | | |
| O(1) – H(1W) ··· N(3) | 0.81(3) | 2.05(3) | 2.852(3) | 171(3) | |
| O(1) – H(2W) ··· N(1) | 0.83(2) | 2.56(3) | 3.212(3) | 137(2) | -x+2, -y+1, -z-1 |
| O(2) – H(3W) ··· N(11) | 0.83(2) | 2.00(2) | 2.796(3) | 162(2) | x, y, z-1 |
| O(2) – H(4W) ··· N(10) | 0.84(3) | 2.02(3) | 2.838(2) | 166(3) | -x+1, -y, -z |
| O(3) – H(6W) ··· N(6) | 0.82(2) | 2.00(2) | 2.799(3) | 167(3) | |
| O(4) – H(7W) ··· N(8) | 0.81(3) | 2.04(3) | 2.837(3) | 170(3) | |
| O(5) – H(9W) ··· N(4) | 0.86(3) | 1.71(3) | 2.568(2) | 170(3) | |
| O(6) – H(12W) ··· N(12) | 0.87(3) | 1.73(2) | 2.597(2) | 173(2) | |
| N(13) – H(13N) ··· O(1) | 0.79(2) | 1.89(2) | 2.668(2) | 169(2) | |
| O(6) – H(13W) ··· N(9) | 0.88(2) | 1.72(2) | 2.589(3) | 170(3) | -x+1, -y, -z |
| N(14) – H(14N) ··· O(2) | 0.81(2) | 1.83(2) | 2.618(2) | 164(3) | |
| N(15) – H(15N) ··· O(3) | 0.81(3) | 1.84(3) | 2.621(2) | 165(3) | |
| N(16) – H(16N) ··· O(4) | 0.85(2) | 1.82(2) | 2.655(2) | 166(2) | |
| *(ampyH$_2$)$_2$[Fe(CN)$_6$]·2H$_2$O (**6**)* | | | | | |
| N(5) – H(1N) ··· O(1) | 0.94(9) | 2.47(8) | 2.935(8) | 111(6) | -x+3, -y+2, -z-1 |
| N(5) – H(1N) ··· N(2) | 0.94(9) | 2.15(9) | 3.000(9) | 151(7) | -x+2, -y+2, -z-1 |
| O(1) – H(1W) ··· N(3) | 0.85(7) | 2.22(9) | 3.006(9) | 154(9) | |
| N(5) – H(2N) ··· N(1) | 0.92(6) | 1.90(6) | 2.821(7) | 175(6) | |

| | | | | | |
|---|---|---|---|---|---|
| O(1) – H(2W) ··· N(2) | 0.79(12) | 2.24(11) | 3.026(10) | 171(10) | -x+2, -y+2, -z |
| N(5) – H(3N) ··· N(3) | 0.92(9) | 1.94(9) | 2.836(9) | 165(8) | x, y, z-1 |
| N(4) – H(4N) ··· N(2) | 0.79(10) | 2.13(10) | 2.900(9) | 167(9) | -x+1, -y+1, -z |
| *$(tptzH_3)_2[Fe(CN)_4(CNH)_2]_3 \cdot 10H_2O$ (**7**)* | | | | | |
| N(1) – H(1N) ··· N(7) | 1.08(18) | 2.0(2) | 2.715(6) | 123(14) | -x+1/2, -y+1/2, -z |
| O(1) – H(1W) ··· N(6) | 0.75(6) | 2.05(6) | 2.793(8) | 171(6) | -x+1, y+1, -z+1/2 |
| O(1) – H(2W) ··· N(2) | 0.80(7) | 1.96(7) | 2.739(6) | 165(6) | x+1/2, y+1/2, z |
| N(3) – H(3N) ··· O(2) | 0.76(7) | 1.87(7) | 2.617(8) | 171(5) | -x+1/2, -y+1/2, -z |
| O(2) – H(3W) ··· N(7) | 0.84(10) | 2.59(9) | 3.322(8) | 146(13) | -x+1/2, -y+1/2, -z |
| O(2) – H(4W) ··· N(2) | 0.84(9) | 2.43(12) | 3.185(8) | 150(13) | |
| O(2) – H(4W) ··· O(1) | 0.84(9) | 2.46(11) | 3.158(9) | 142(14) | x-1/2, y+1/2, z |
| O(3) – H(5W) ··· N(5) | 0.80(6) | 2.01(6) | 2.799(6) | 176(7) | x+1/2, y+1/2, z |
| O(3) – H(6W) ··· N(7) | 0.92(7) | 2.23(8) | 3.130(6) | 167(7) | |
| O(4) – H(7W) ··· N(4) | 0.87(5) | 2.53(5) | 3.370(9) | 164(6) | |
| N(8) – H(8N) ··· O(4) | 1.24(10) | 1.32(11) | 2.533(7) | 165(9) | |
| O(4) – H(8W) ··· N(4) | 0.85(3) | 1.83(5) | 2.654(6) | 163(9) | -x+1/2, -y-1/2, -z |
| O(5) – H(10W) ··· N(6) | 0.86(4) | 2.07(3) | 2.884(6) | 158(5) | |
| N(11) – H(11N) ··· O(3) | 0.94(6) | 1.77(5) | 2.716(6) | 177(6) | x-1/2, y+1/2, z |
| N(13) – H(13N) ··· O(1) | 0.85(5) | 1.87(5) | 2.663(6) | 155(4) | |
| N(15) – H(15N) ··· O(5) | 0.91(7) | 1.81(7) | 2.693(5) | 163(7) | |
| *$(tptzH_3)[Fe(CN)_6] \cdot 3H_2O$ (**8**)* | | | | | |
| O(1) – H(1W) ··· N(3) | 0.87(3) | 2.35(5) | 3.036(5) | 136(4) | -x+1/2, -y+1/2, -z+1 |
| O(1) – H(2W) ··· N(2) | 0.85(6) | 1.95(6) | 2.759(5) | 159(6) | -x+1, -y+1, -z+1 |
| O(2) – H(3W) ··· N(2) | 0.9000 | 2.4200 | 3.273(7) | 160.00 | |
| N(6) – H(6N) ··· O(1) | 0.87(5) | 1.84(5) | 2.680(5) | 162(5) | -x+1/2, -y+3/2, -z+1 |

| | | | | | |
|---|---|---|---|---|---|
| N(7) – H(7N) ··· N(1) | 0.8600 | 2.3100 | 2.892(5) | 125.00 | x+1/2, y-1/2, z |

### 3.2 Description of the Structures

*3.2.1 $(bpyH_2)_2[Fe(CN)_6]\cdot 2H_2O$ (**1**).*

Compound **1** crystallizes in the monoclinic space group C2/m with a quarter of the octahedral $[Fe(CN)_6]^{4-}$ anion, a half of a $bpyH_2^{2+}$ cation, and a half of a water molecule in the asymmetric unit.

The coordination polyhedron about Fe(II) is almost ideal due to symmetry, with the minor distortions better seen from the variation of the Fe – C bond distances which are 1.911(5), 1.910(5) and 1.896(5) Å.

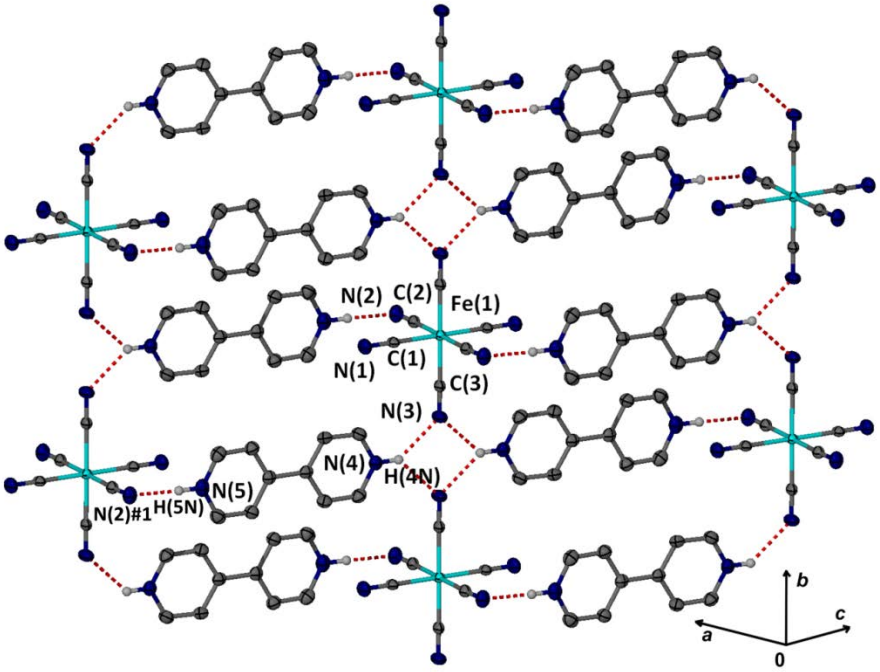


**Figure 1.** A part of the H-bonded 2D sheet formed in the crystal of **1** due to the interactions between anions and cations with a partial labelling scheme. Ellipsoids are drawn at the 40 % level and C-H hydrogen atoms are omitted for clarity. Symmetry operation: #1, -x+1/2, y-1/2, -z-1.

The crystal structure is dominated by a network of H-bonds which include the 4,4'-bpy N atoms and the water O atoms as donors, and the coordinated cyanide N atoms as acceptors. One of the pyridinium rings acts as a donor to two symmetry related cyanides belonging to two adjacent $[Fe(CN)_6]^{4-}$ anions forming a bifurcated H-bond (the sum of the angles about H4N is 358,35 $^{o}$), while the other pyridinium ring forms a simple H-bond to a different cyanide. This way a 2D sheet is formed parallel to the (2 0 1) plane of the cell. (Fig 1).

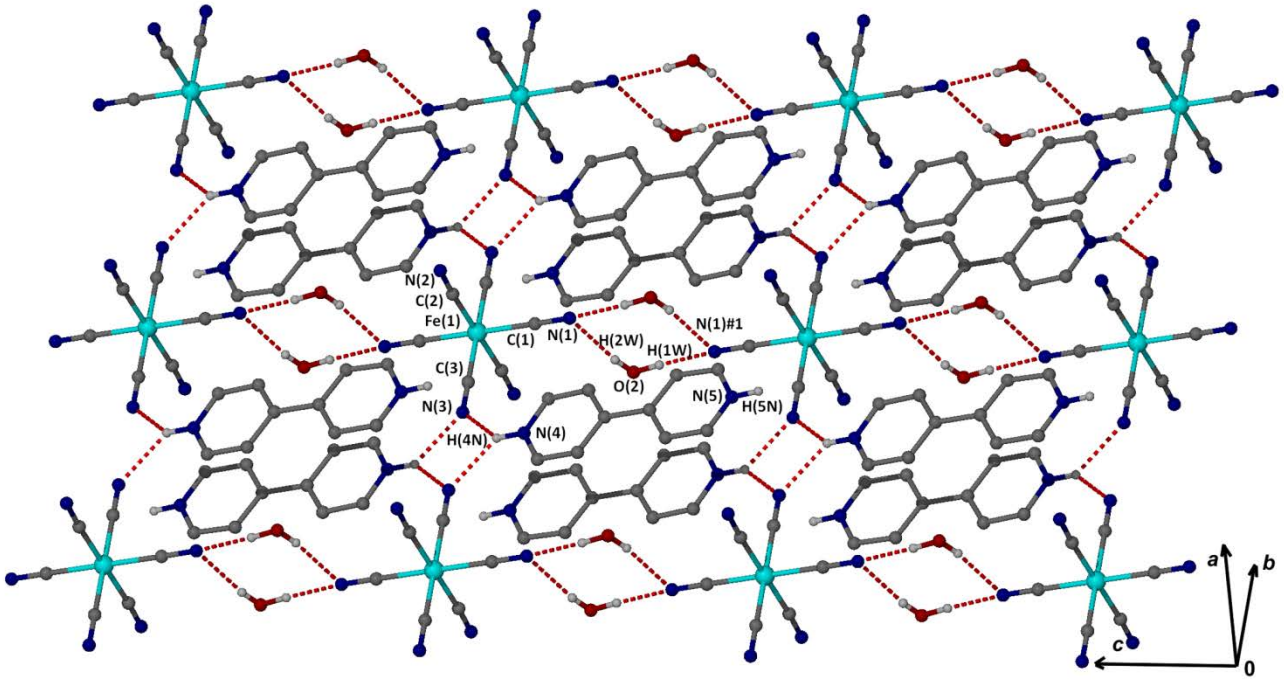


**Figure 2.** The connection of the $[Fe(CN)_6]^{4-}$ anions by water molecules which leads to 2D sheets. Symmetry operation: #1, -x, y, -z-1.

The "free" NH [N(5)-H(5N)] interacts with N(2) above and below the presented sheet (as in Fig. 1) to form a 3D architecture.

There is a stacking interaction between heterocyclic cations belonging to different sheets. $bpyH_2^{2+}$ cations are parallel with the ring containing N(4) opposite to a ring

containing N(5) related by the –x-1/2, y+1/2, -z-1 symmetry operation. The distance of the best calculated planes is 3.51(1) Å while there is a significant offset towards the adjacent ring (1.97(1) Å).

Those 2D sheets are also connected with double water bridges, as shown in Figure 2, leading to the formation of a 3D supramolecular architecture.

Topologically a binodal net is formed; $bpyH_2^{2+}$ is a three – connected node interacting with three anions, while $[Fe(CN)_6]^{4-}$ is an eight – connected node interacting with six cations and two anions via the water bridges. The network has a total point symbol $[4^3]_2[4^6.6^{18}.8^4]$ and belongs to the **tfz-d** type. (Fig. 3)

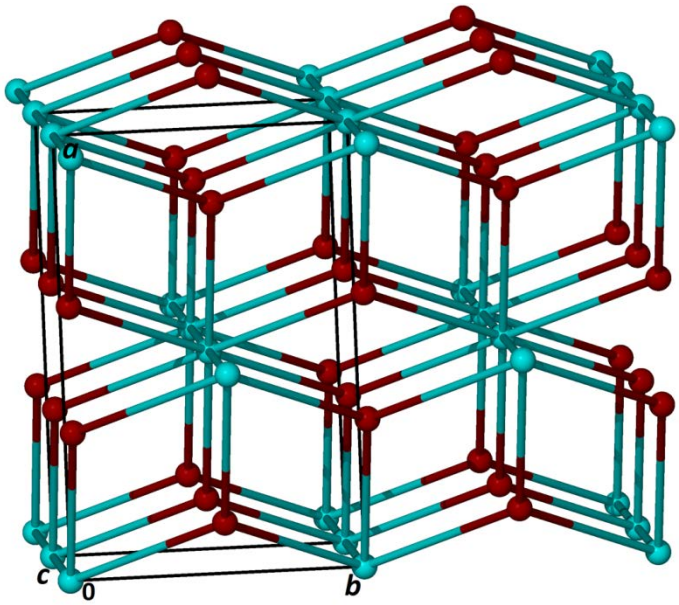


**Figure 3**. The tfz-d network formed in the structure of **1**. Sky blue spheres are the Fe(II) atoms while the centroids of the $bpyH_2^{2+}$ cations are shown as red spheres.

There is a handful of bpy cations in cyanometallate chemistry. Monoprotonated bpy does not interact with anions but forms 1D chains via N-H-N bridges. $bpyH_2^{2+}$ can form two bifurcated H-bonds in an anhydrous tetracyanoplatinate, [3d] or a $[bpyH_2(H_2O)_2]^{2+}$ complex

which is connected to $[Pt(CN)_4]^{2-}$ [3d] or to $[W(CN)_8]^{4-}$.[21] Our case is the first with three H-bonds from $bpyH_2^{2+}$.

*3.2.2 $(bpyH_2)(H_3O)[Fe(CN)_6]$ (**2**).*

Compound **2** crystallizes in the monoclinic space group $P2_1$ with one distorted octahedral anion $[Fe(CN)_6]^{3-}$, one $bpyH_2^{2+}$ and one hydronium cations in the asymmetric unit. The Fe-C distances in the anion span the range 1.929 – 1.948 Å, while the distortion is better seen by the deviation from 90 and 180 ° of the cisoid and transoid angles, respectively. The 4,4'-bipyridinium cation is twisted with the dihedral angle between the pyridinium rings being 39.59(1)°.

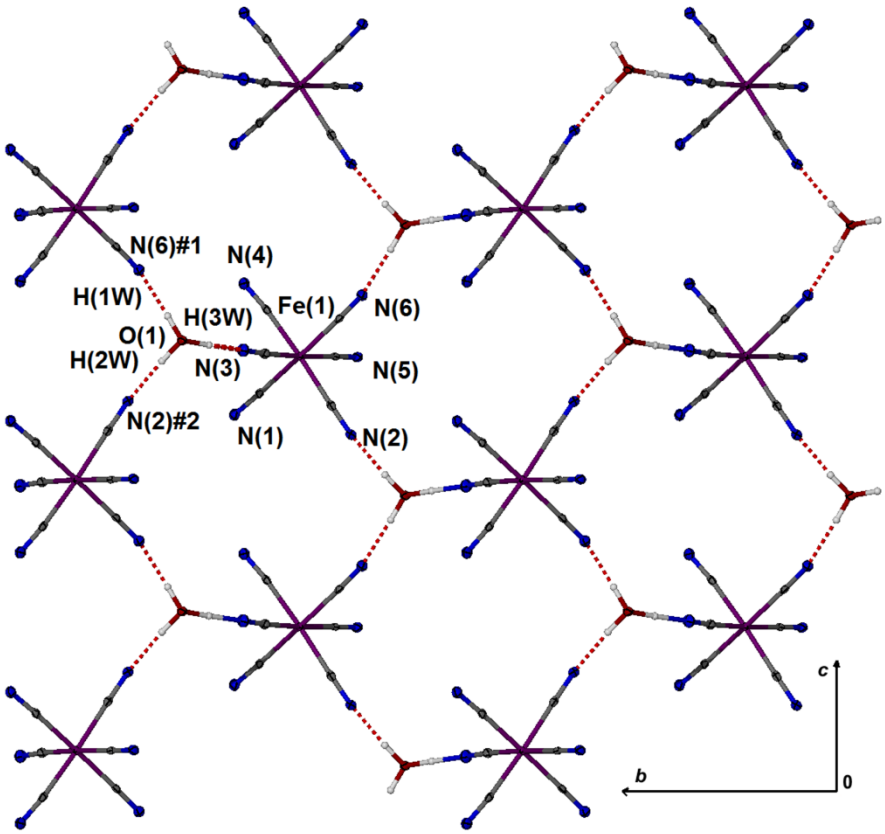


**Figure 4.** A part of the undulating (6,3) net formed in **2** by $[Fe(CN)_6]^{3-}$ and $H_3O^+$ interactions parallel to *bc* plane. A partial labelling scheme is included and ellipsoids are drawn at 50 % probability level. Symmetry operations: #1, -x+1, y+1/2, -z+1; #2, -x+1, y+1/2, -z.

Each hydronium participates in three different H-bonds as donor to three different anions, being responsible for the formation of a (6,3) 2D network. (Fig. 4)

This way the three cyanides [N(2), N(3), N(6)] occupying a trigonal face of the octahedral anion are H-bonded to a hydronium. The other three [N(1), N(4), N(5)], in addition to hydronium's O(1), act as acceptors for H-bonding with the organic cation. One of $bpyH_2^{2+}$ rings is accommodated into the hexagonal cavities of the net described above, and forms a H-bond with an anion belonging to an adjacent 2D sheet. [N(7)-H(7N)···N(5)#3] The

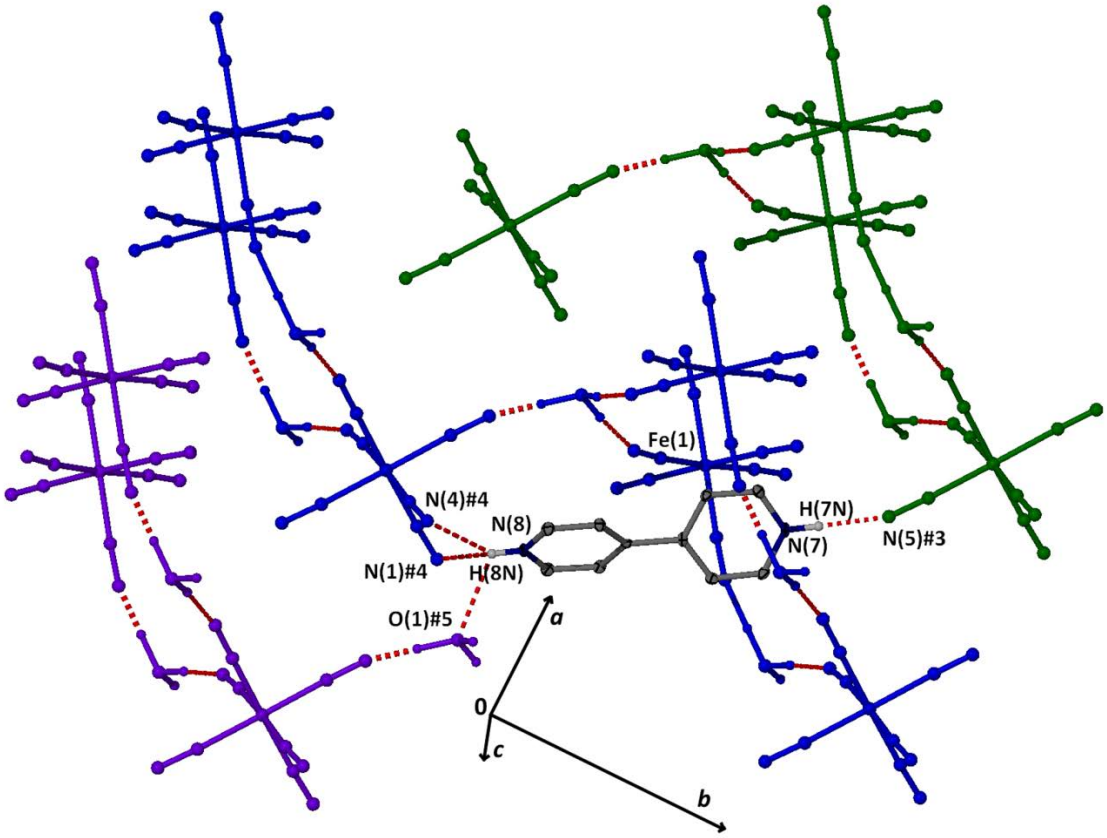


**Figure 5.** The interaction of $bpyH_2^{2+}$ with three different anionic layers in **2**. Only one cation is shown for clarity. Symmetry operations: #3, -x+2, y+1/2, -z; #4, -x+1, y-1/2, -z; #5, -x, y-1/2, -z.

other ring is involved in a trifurcated H-bond. Two of the components are directed to an anion belonging to the same sheet while the third component to a hydronium belonging to a 2D layed other that the former. This way a bipyridinium cation connects three different anionic sheets.

It is rather difficult to describe topologically the supramolecular architecture formed in **2** taking into account all interactions. To simplify the procedure, the two weaker components of the trifurcated H-bond can be neglected. This leads to a uninodal net; both ferricyanide and hydronium are four connected nodes since each one interacts with three others directly through H-bonds plus one indirect interaction via bipyridinium. This connectivity scheme leads to two interpenetrated nets with **cds** topology (Fig.6); the point symbol is $[6^5.8]$.

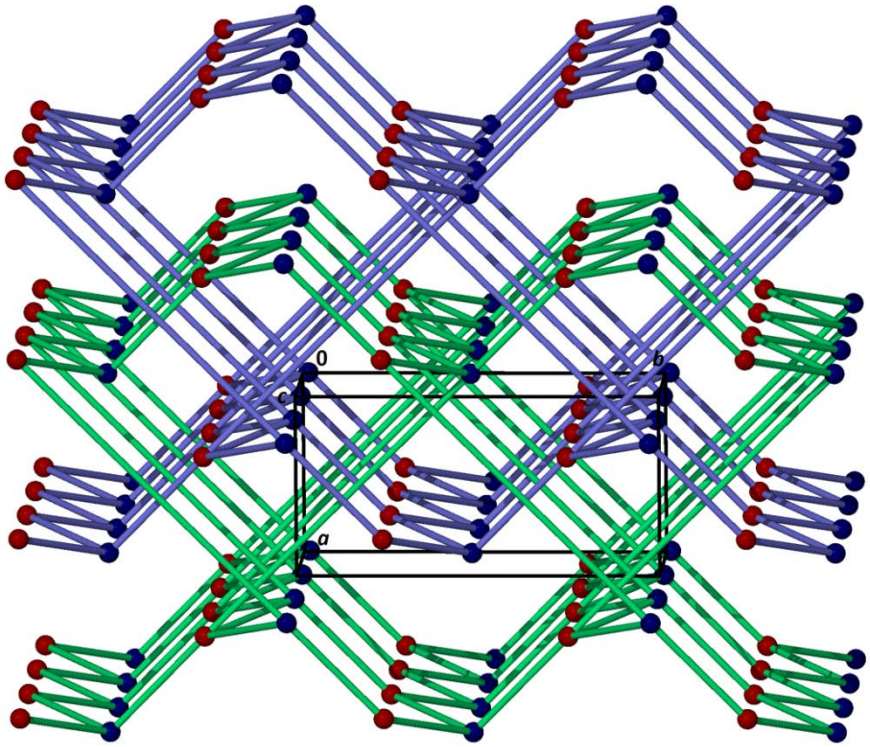


**Figure 6.** The very distorted **cds** topology of the network formed in **2**. Blue and red spheres represent Fe(III) and oxonium O atoms, respectively.

*3.2.3 ($bpeH_2$)($H_3O$)[$Fe(CN)_5(CNH)$]·$H_2O$ (**3**)*

Compound **3** is crystallized in the monoclinic space group Ia with one $[Fe(CN)_5(CNH)]^{3-}$ anion, one $bpeH_2^{2+}$ and one oxonium cations and a disordered water molecule in the asymmetric unit.

The coordination sphere of the hydrohexacyanoferrate(II) anion is slightly distorted. Five Fe-C distances are very close spanning the range 1.909 – 1.915 Å while the sixth (*trans* to Fe-CNH) is noticeably shorter. Previous findings suggest that both Fe-C and C≡N bonds are shorter in dihydrohexacyanoferrates [22] and in ferro- [23] and ferri- [24] cyanic acids. Our data are in agreement with the latter but oppose the former. This is probably due to the fact that the Fe-C-N angle in our case of Fe-CNH bonding is significantly smaller (175.9(4) °) than 180 °. This probably reduces the strength of π-bonding involved in the interaction Fe-CNH.

In addition to the CNH group that acts as a donor to the lattice water molecule, four of the cyanides act as acceptors in H-bonds with water and oxonium. (Fig. 7)

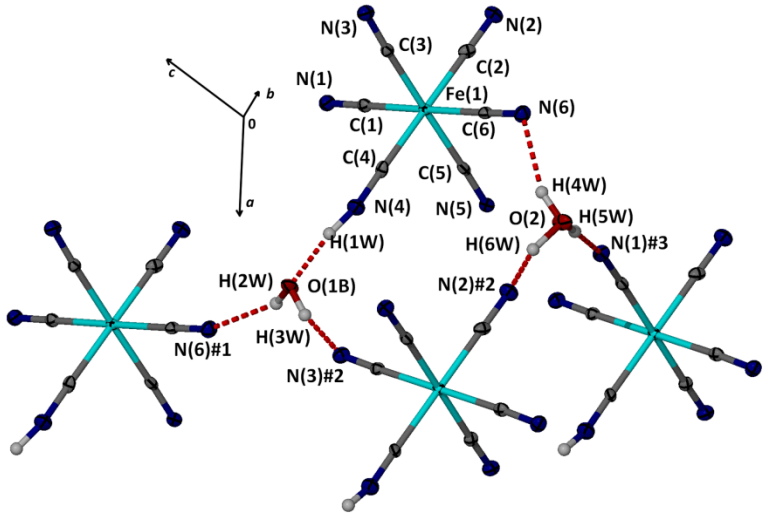


**Figure 7.** A diagram showing the H-bonds responsible for the 3D network in **3**. Only one part of the disordered water molecule is shown for clarity. Symmetry operations: #1, x+1/2, y-1/2, z+1/2; #2, x+1/2, -y+2, z; #3, x, -y+3/2, z-1/2.

Zig-zag chains running along *a* are formed by alternating hydrohexacyanoferrates and pairs of water and oxonium moieties. The H-bonds responsible for these chains are: O(2)-H(4W)···N(6), O(2)-H(6W)···N(2)#2, N(4)-H(1W)···O(1) and O(1)-H(3W)···N(3)#2. The other two H-bonds, O(1)-(H2W)···N(6)#1 and O(2)-H(5W)···N(1)#3 connect each chain to four neighboring chains, as shown in Fig. 8. The $bpeH_2^{2+}$ cations are lying parallel to the (2 0 1) dimension of the cell, and they are connected to the network by two H-bonds, namely N(7)-H(7N)···N(5) and N(8)-H(8N)···N(1).

Topologically, the oxygen atoms can be considered as 3-connected nodes while the iron complex is 8-connected or 6-connected node depending on the presence or not of $bpeH_2^{2+}$ as a linker. In both cases the topological types are new and the point symbols are

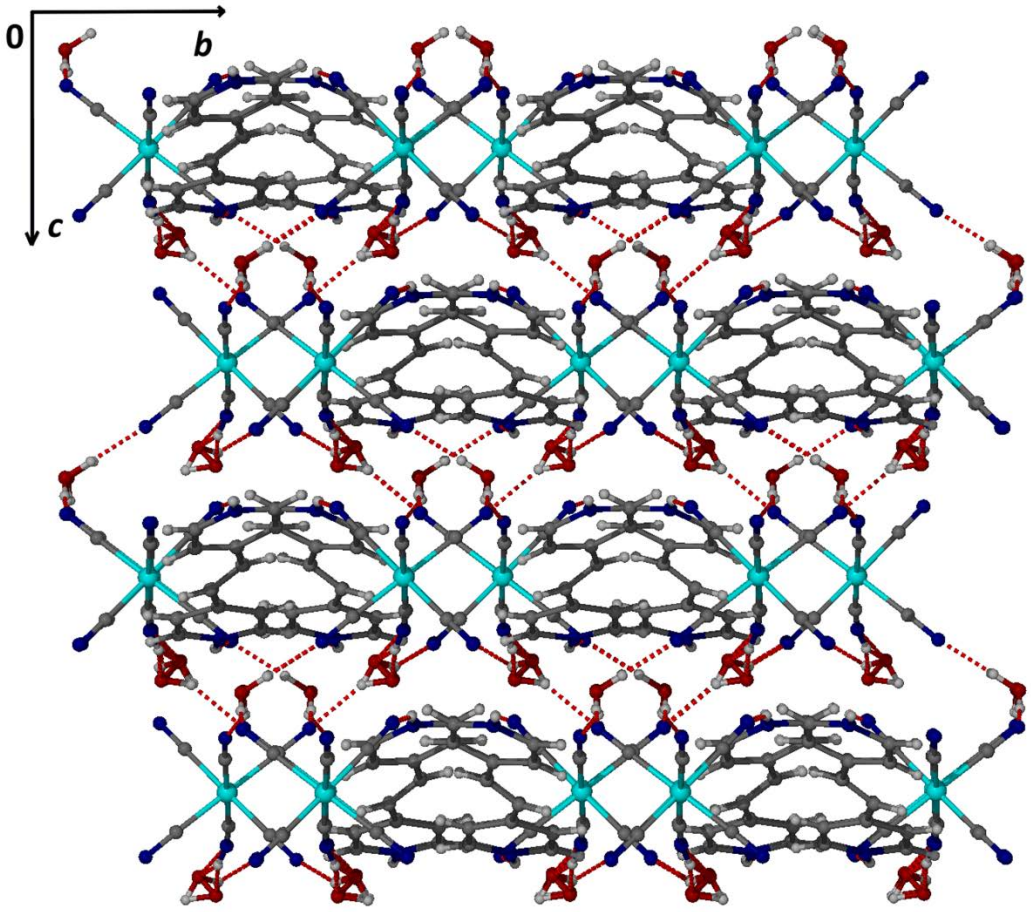


**Figure 8.** A packing diagram of **3** down to *a* axis.

$[4^2.6]_2[4^4.5^8.6^{10}.7^5.9]$ and $[4^2.6]_2[4^4.6^2.8^7.10^2]$ for the two scenarios, respectively.

*3.2.4 $(bpeH_2)(H_5O_2)[Fe(CN)_6]\cdot 2H_2O$ (**4**)*

Compound **4** is crystallized in the monoclinic space group C2/c. Present in the unit cell are a ferricyanide anion, a $bpeH_2^{2+}$ and a linear $H_9O_4^+$ cations. The water molecules at the edges of the tetraaqueous cation are disordered. The coordination sphere about Fe(III) is slightly distorted with the Fe-C distances being 1.935(3) and 1.942(3) Å, while all the *cis* angles are in the range 89.92 – 93.41 °.

The cation consists of a hydrogen atom that bridges two water molecules and those are H-bonded to two more water molecules. Three hydrogen atoms of the $H_9O_4^+$ species are used for intra-ion H-bonds and the rest are interacting with six different anions, as shown in

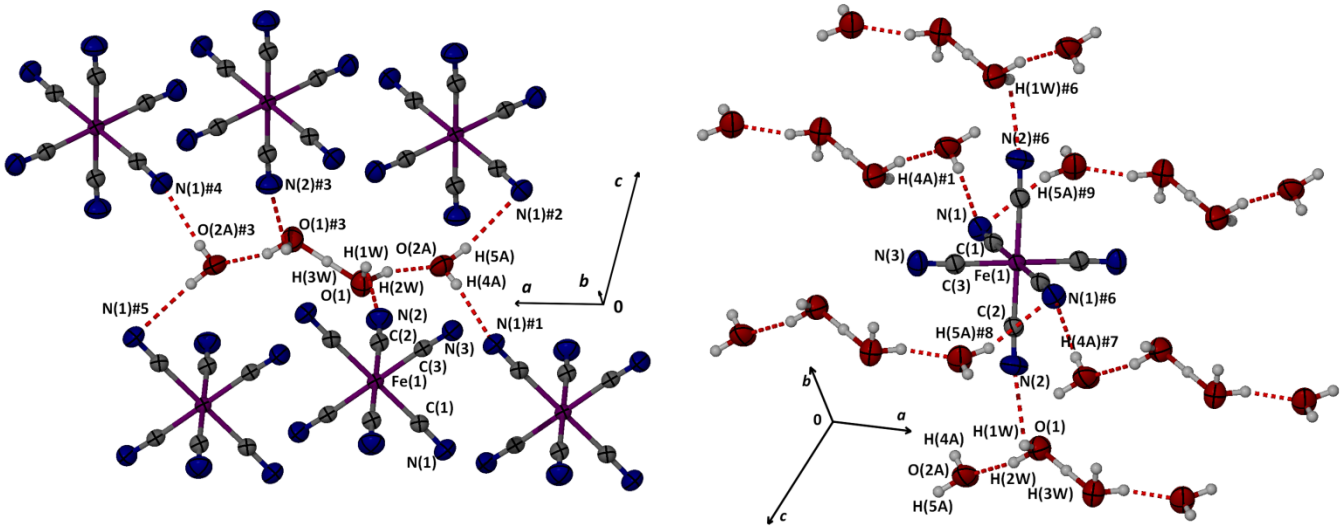


(a) (b)

**Figure 9.** H-bonding interactions between $[Fe(CN)_6]^{3-}$ and $H_9O_4^+$. The connectivities of the cation (a) and anion (b) are shown. Thermal ellipsoids are at the 50% probability level. Symmetry operations: #1, -x, -y+1, -z; #2, x, -y+1, z+1/2; #3, -x+1, y, -z+1/2; #4, x+1, -y+1, z+1/2; #5, -x+1, -y+1, -z; #6, -x+1/2, -y+3/2, -z; #7, x+1/2, y+1/2, z; #8, -x+1/2, y+1/2, -z+1/2; #9, x, -y+1, z-1/2.

Fig. 9a. The shape of the polyhedron formed if we consider the iron(III) atoms as vertices resemples a trigonal prism.

Each $[Fe(CN)_6]^{3-}$ anion utilizing four equatorial cyanides for interaction with the cations. N(1) is connected to two cations while N(2) to one. N(3) remains for the N(4)-H(4N)···N(3) interaction which connects $bpeH_2^{2+}$ to the 3D network eventually formed. $bpeH_2^{2+}$ is parallel to the (1 0 1) direction of the cell. A packing diagram is shown in Fig. 10.

The shape of the polyhedron about the anion, if we consider as vertices the centroids of the cations, is octahedral. This explains the topology of the network formed (ignoring the heterocyclic cation). The network is 6-connected binodal (with octahedral and trigonal prismatic nodes) with **nia** (NiAs) topology and point symbol $[4^{12}6^3][4^9.6^6]$. (Fig. 11)

$bpeH_2^{2+}$ has been used rather extensively as a supramolecular tecton in crystal engineering. It has been found as a counter ion in cyanides, [25] chlorides, [26] other anionic metal complexes [27] and organic salts.[28] To our surprise, there is an $bpeH_2^{2+}$

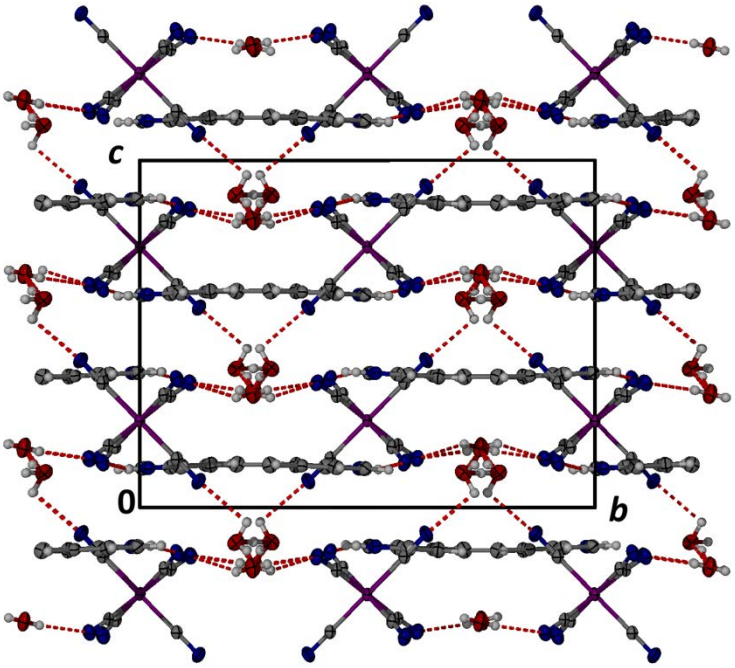


**Figure 10.** A packing diagram of **4** showing the position of $bpeH_2^{2+}$ in the cell, relatively to the positions of other species.

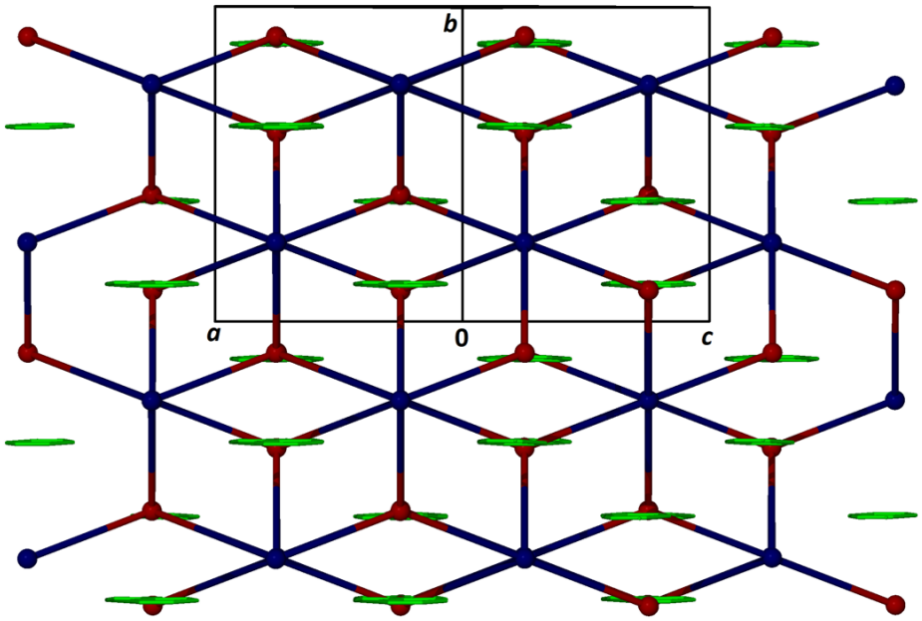


**Figure 11**. The **nia** topology present in the crystal structure of 4. Blue and red spheres are respectively the centroids of the anion and tetra-aqueous cation while with green is denoted the position of the heterocyclic cation.

hexacyanoferrate which, with minor differences, looks the same with **4**. Careful examination reveals that Maji's [12] compound is formulated as $(bpeH_2)(H_3O)_2[Fe(CN)_6]\cdot 2H_2O$ while ours $(bpeH_2)(H_5O_2)[Fe(CN)_6]\cdot 2H_2O$.

*3.2.5 $(dabcoH_2)(H_3O)[Fe(CN)_6]\cdot 2H_2O$ (**5**)*

Compound **5** is crystallized in $P\bar{1}$ space group, and while it is formulated as $(dabcoH_2)(H_3O)[Fe(CN)_6]\cdot 2H_2O$, in the asymmetric unit there are pairs of ferricyanide anions, hydroniums and H-bonded diazabicyclooctanium – water complexes with very small structural differences.

The geometry about Fe(III) is slightly distorted and the Fe-C bond distances span the range 1.935 – 1.951 Å.

The 3D architecture formed in the crystal is rather complicated since it is obvious that there are three different species able to behave as nodes in a network. Starting from the cations, each hydronium is connected to three different anionic complexes and each Fe(III) complex is connected to three hydroniums. $[Fe(CN)_6]^{3-}$ are utilizing three meridional cyanides as acceptors, and the 2D network formed is almost planar (Fig. 12).

Protonated dabco does not interact with anionic complexes. It participates as donor to two H-bonds to two lattice water molecules, and the supramolecular complex formed interacts as donor with four ferricyanides, as shown in Fig. 13. Three of the H-bonds are directed towards the cyanides occupying meridional positions and are not involved in the

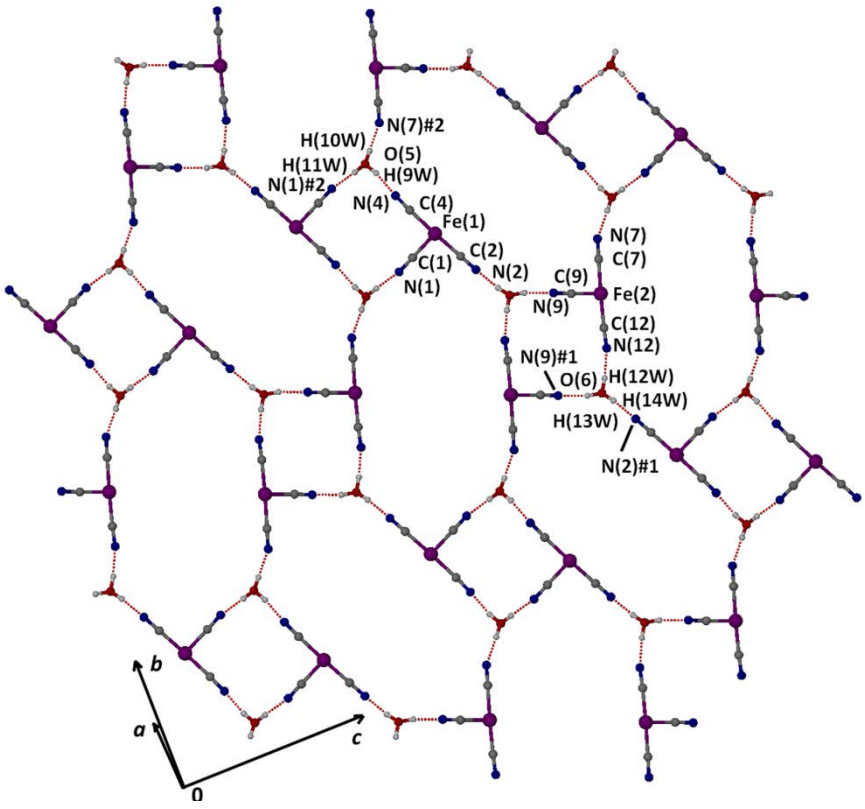


**Figure 12.** The anionic plane net formed in **5** by the interaction of $H_3O^+$ with $[Fe(CN)_6]^{3-}$. Only the interacting cyanides are shown for clarity. Symmetry operations: #1, -x+1, -y, -z; #2,-x+3, -y+1, -z-1.

formation of the 2D sheet described above. The last proton is directed between two cyanides already used from the oxonium ions for H-bonds. The interaction is weak, but the sum of the angles about hydrogen atom is very close to 360 º indicating bifurcated bond.

As shown in Fig. 12, the 2D architecture is based on 8- and 4-membered rings (considering nodes). Pairs of dabco supramolecular complexes are located into the 8-membered rings and each one of them interacts with three ferricyanides of the same layer, and one belonging to a different layer. This way, a pair $dabcoH_2^{2+}$ cations, contained in

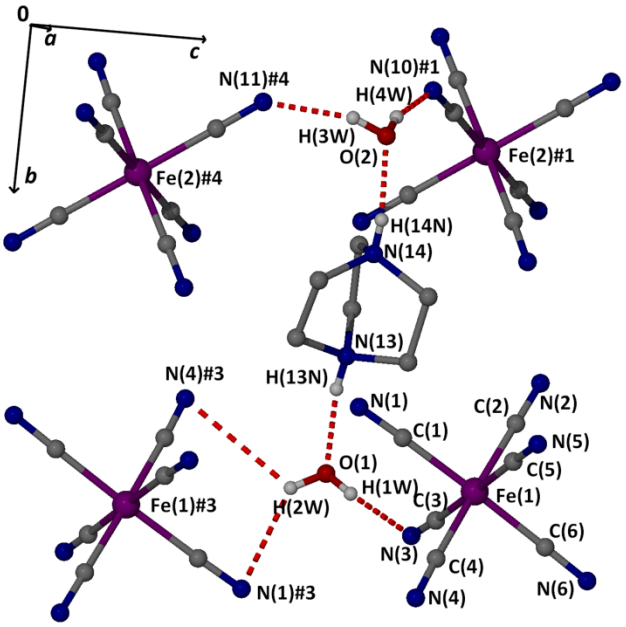


**Figure 13.** The connection of $dabcoH_2^{2+}$ with two water molecules for the formation of a supramolecular complex and its interactions with four $[Fe(CN)_6]^{3-}$ anions. The second dabco complex has very similar structural characteristics and interactions. : #1, -x+1, -y, -z; #3, -x+2, -y+1, -z-1; #4, x, y, z-1.

the same cavity, connects three successive layers, built from the interactions of ferricyanides with oxoniums. (Fig. 14) The bifurcated H-bond is directed to cyanides above and bellow the 4-membered rings.

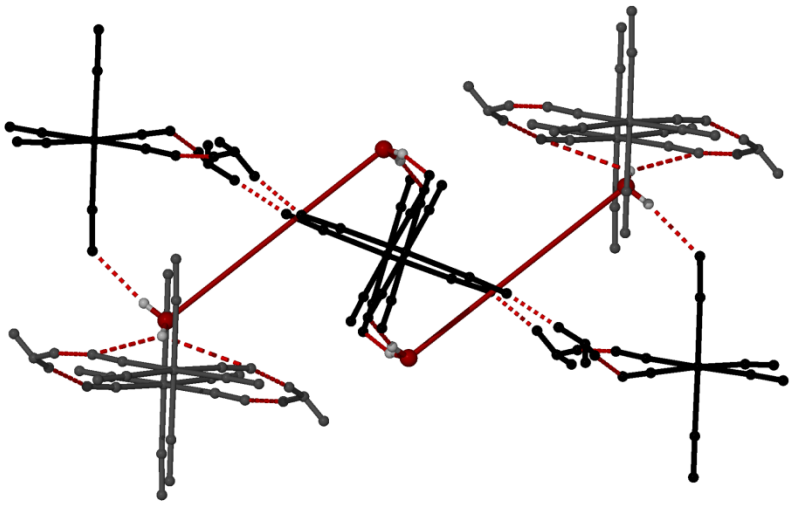

**Figure 14.** A schematic diagram showing the interactions of dabco$H_2(H_2O)_2$ complex (red bars) with different (black and grey) $[Fe(CN)_6]^{3-}$-$H_3O^+$ layers.

*3.2.6 ($ampyH_2)_2[Fe(CN)_6]\cdot 2H_2O$ (**6**)*

Compound **6** crystallizes in the monoclinic space group $P\bar{1}$ with one half ferrocyanide, one 4-ammoniummethylpyridinium dication and one water molecule in the asymmetric unit.

All N-H bonds are involved in H-bonding leading to a 3D supramolecular architecture. The methylammonium group (N(5)) is connected to three anions (interacting with N(1), N(2) and N(3)) while each anion is connected to six $ampyH_2^{2+}$ cations , forming a dual kagome plane net parallel to the *bc* plane of the cell. (Fig.15a) The pyridinium cations are alternatively pointing above and below the plane net, and interact with cyanides [N(4)-H(4N)···N(2)(-x+1, -y+1, -z)] (N(2) is the acceptor of H-bonds from methylammonium, pyridinium and water as well) belonging to different layers, expanding the architecture to the third dimension. The overall topological type is **flu** (fluorite) since the cation as node has increased its coordination number by one and the anion by two, due to the participation of pyridinium. (Fig. 16)

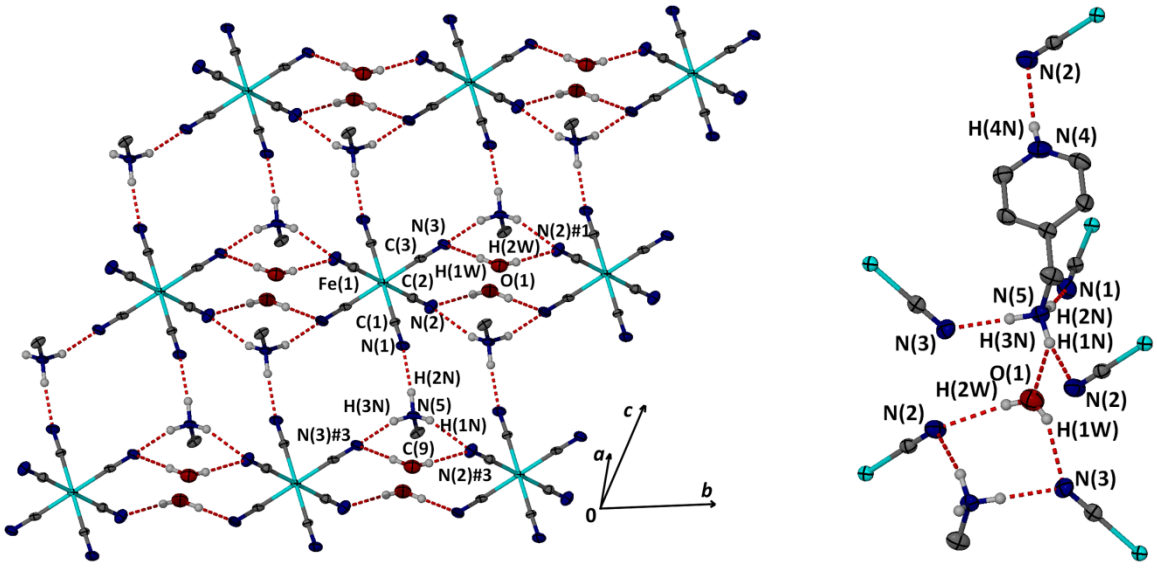


(a) (b)

**Figure 15.** a) The H-bonding interactions leading to the formation of 2D sheets parallel to *bc* plane in **6**; the lattice water molecule is also included. The methylene carbon indicates the direction of the pyridinium ring relative to the layer. b) All hydrogen bonds formed in **6**. Symmetry operations: #1, -x+2, -y+2, -z; #2, x, y, z-1; #3, -x+2, -y+2, -z-1; #4, -x+1, -y+1, -z; #5 –x+3, -y+2, -z-1.

The water molecule is held in the network forming three H-bonds, two as donor and one as acceptor. As a donor is bonded to two cyanides (N(2) and N(3)) belonging to adjacent ferrocyanides of the same dual kagome layer. One of the methylammonium hydrogen atoms (H(1N)) is forming a bifurcated H-bond (sum of surrounding angles: 359.64 $^{o}$). One of the components is directed towards a cyanide, as shown in Fig. 15, and the other component towards a water molecule belonging in a different **kgd** net. The H-bonds of all donors are presented in Fig. 15b.

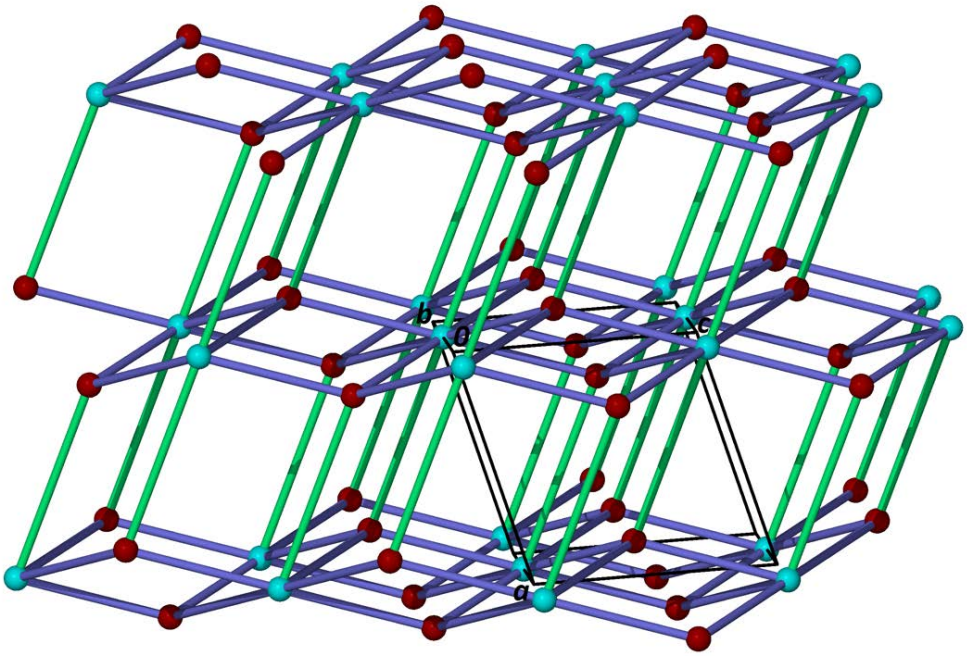


**Figure 16.** The **flu** network formed in the structure of **6**. Sky blu and red spheres represent the centroids of the anion and cation, respectively. The interactions of the methylamonium group of the cations are represented by purple bars, while the pyridinium interactions of the cations are represented by green bars.

*3.2.7 $(tptzH_3)_2[Fe(CN)_4(CNH)_2]_3 \cdot 10H_2O$ (**7**)*

Compound **7** is crystallized in the monoclinic space group C2/c. Its asymmetric unit contains one *cis*-dihydrohexacyanoferrate(II) anion, one half of a *trans*-dihydrohexacyanoferrate anion, one $tptzH_3^{3+}$ cation and five water molecules.

Both coordination spheres of Fe(1) and Fe(2) are distorted with Fe – C bond lengths in the range 1.864 – 1.925 Å, with the shorter bond lengths belonging to the coordinated hydrocyanates.

All non C-H protons are involved in H-bonding. To realize the supramolecular architecture is useful to proceed step by step.

a) The dihydrohexacyanoferrates interact with three of the available water molecules, namely O(2), O(3) and O(4), and they form a 2D layer parallel to the *ab* plane of the cell.

Water O(2) bridges two adjacent "*cis*" anions {N(3)-H(3N)···O(2)(-x+1/2, -y+1/2, -z) and O(2)-H(4W)···N(2)} and the dimer in turn is connected to two "*trans*" anions by a hydrogen bridge N(1)-H(1N)···N(7)(-x+1/2, -y+1/2, -z) and water O(4) {O(4)-H(7W)···N(4) and N(8)-H(8N)···O(4)}. This way a chain formed, running parallel to the (0 2 0) direction of the cell, consisted of alternating pairs of "*cis*" Fe(1) and single "*trans*" Fe(2) anions. The "*trans*"

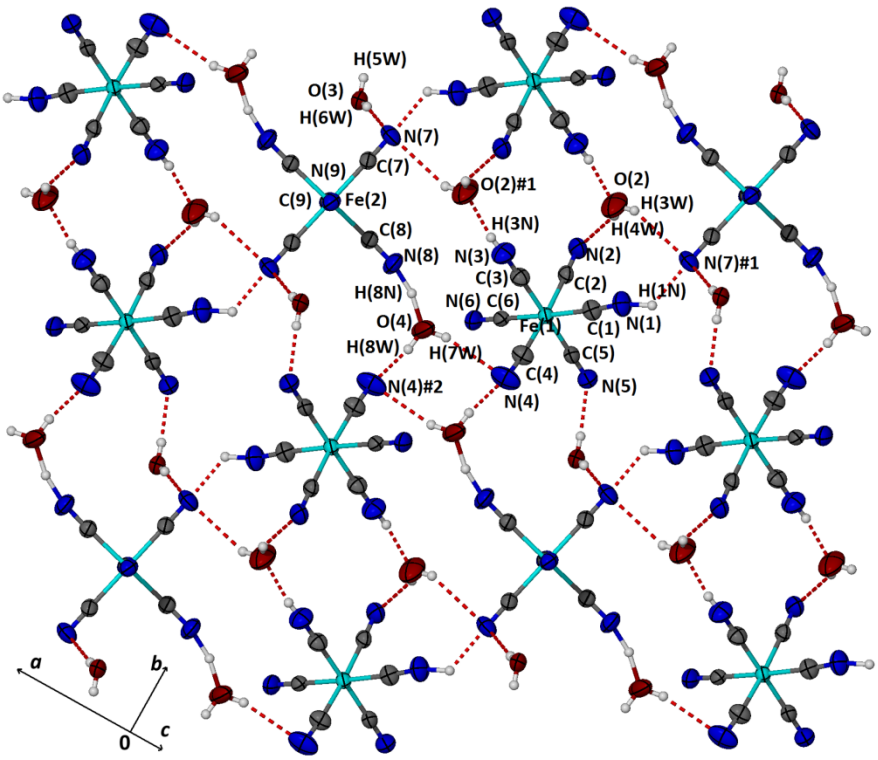


**Figure 17.** A view of the 2D layer formed in **7** parallel to *ab*. Symmetry operations: #1, -x+1/2, -y+1/2, -z; #2, -x+1/2, -y-1/2, -z.

Fe(2) anions are also connected to the former dimer with H-bonds from the second proton of water O(2) {O(2)-H(3W)···N(7)(-x+1/2, -y+1/2, -z)}. O(3) is H-bonded out of the chain

{O(3)-H(6W)···N(7)} and with O(4) {O(4)-H(8W)···N(4)(-x+1/2, -y-1/2, -z) are connecting the 1D chains and form the 2D layer parallel to the *ab* plane of the cell. (Fig. 17)

b) Water molecules O(1) and O(5) are connecting the layers described in (a) and form a 3D anionic network. Both of them form interlayer H-bonds with each one of the protons interacting with a different layer. (Fig. 18)

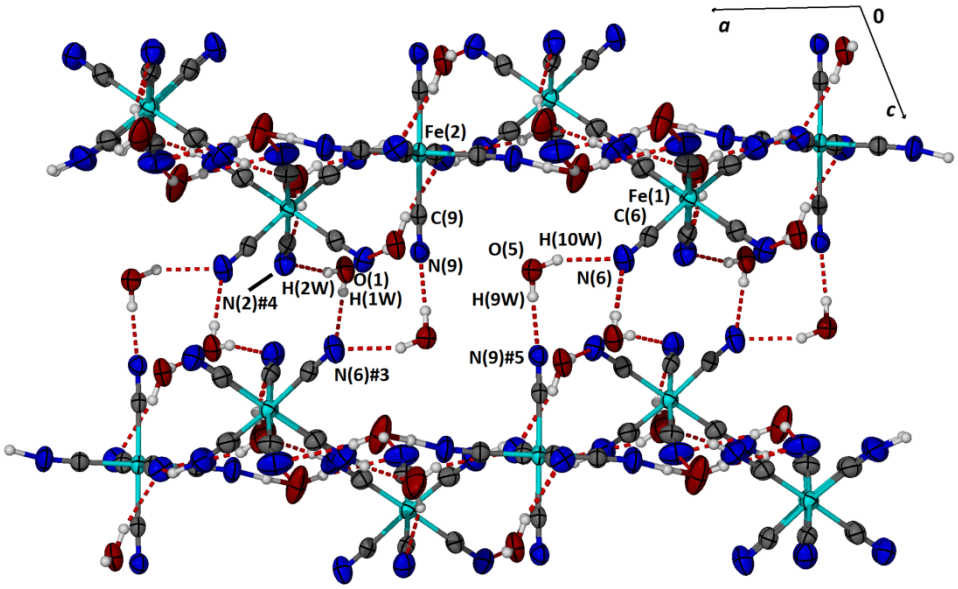


**Figure 18.** A view of the anionic 3D network formed in **7** down to *b* axis, showing how the water molecules O(1) and O(5) connect adjacent layers. Symmetry operations: #3, -x+1, y+1, -z+1/2; #4, x+1/2, y+1/2, z; #5, -x+1, y, -z+1/2.

c) $tptzH_3^{3+}$ cation is connected to the 3D anionic network via H-bonds to three water molecules. Two of these bonds are towards the O(1) and O(5) which connect the two layers described in (a) via N(13)-H(13N)···O(1) and N(15)-H(15N)···O(5), while the third is with O(2) belonging to a layer {N(11)-H(11N)···O(3)(x-1/2, y+1/2, z). A double layer, consisting of $tptzH_3^{3+}$ cations is formed. (Fig. 19)

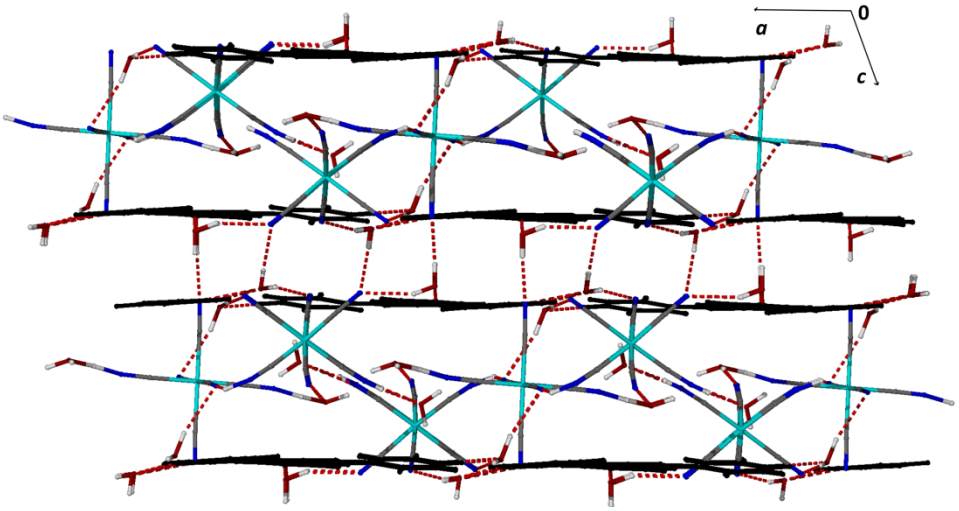


**Figure 19.** A packing diagram of **7** showing the position of the $tptzH_3^{3+}$ (black) cations between anionic layers.

*3.2.8 ($tptzH_3$)[$Fe(CN)_6$].3$H_2O$ (**8**)*

Compound **8** is crystallized in the monoclinic space group C2/c with one half of a $[Fe(CN)_6]^{3-}$ anion, one half of a $tptzH_3^{3+}$ cation and one and a half water molecules.

The inorganic anion show the smallest distortion from ideal octahedral geometry when compared to the previous compounds with the Fe-C bond lengths being in the range 1.936 – 1.950 Å and the *cis* angles in the range 89.91 – 92.21 °; the *trans* are 180 ° due to symmetry. There is a $C_2$ axis passing through one triazine and one pyridinium nitrogen atoms. All pyridinium planes are slightly twisted relatively to the triazine plane with the dihedral angles being 9.42(1) and 19.13(1) ° for rings containing N(6) and N(7), respectively.

Though there are two different water molecules in the crystal structure, only one is active in the 3D framework formed eventually. The water molecule with half occupancy, O(2), is loosely connected to the anions of the network and will be ignored from further discussion.

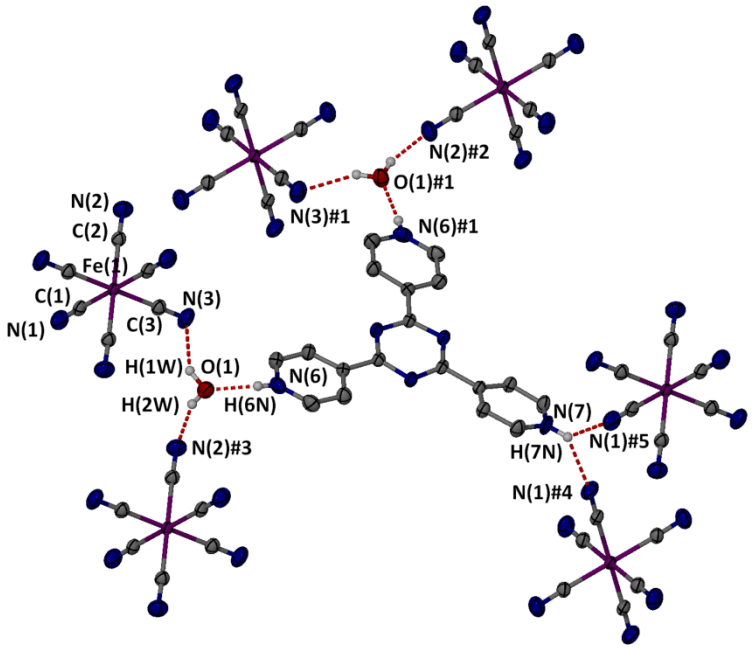


**Figure 20.** The H-bonds present in **8**, and the connectivity of $tptzH_3^{3+}$. Symmetry operations: #1, -x+1, y, -z+1/2; #2, -x+3/2, y-1/2, -z+1/2; #3, x-1/2, y-1/2, z; #4, -x+1/2, y-3/2, -z+1/2; #5, x+1/2, y-3/2, z.

O(1) is connected to a pyridinium ring increasing the ability of $tptzH_3^{3+}$ for H-bonds. A supramolecular complex is present in the structure formulated as $[tptzH_3(H_2O)_2]^{3+}$ which interacts with six different hexacyanoferrate(III)anions, as shown in Fig. 20. Each N-H···$OH_2$ fragment is a donor to two H-bonds directed towards two symmetry related inorganic anions. The third N-H moiety is involved in a bifurcated H-bond connecting two more ferricyanides to the supramolecular complex via N(7)-H(7N)···N(1) interactions

Each $[Fe(CN)_6]^{3-}$ anion is H-bonded with four water molecules in the equatorial plane and the axial positions are forming the N-H···N H-bonds. Considering the $[tptzH_3(H_2O)_2]^{3+}$ and $[Fe(CN)_6]^{3-}$ complexes as 6-connected nodes a new topological net is formed which is self - penetrated [29] with point symbol $[4^6.6^4.8^5][4^6.6^8.8]$.

The mean planes of the $tptzH_3^{3+}$ cations are parallel in the crystal and all of the pyridinium rings are weakly stacked. Triplets of rings are formed with the ring containing N(6) in the middle of two symmetry related rings containing N(7). The mean distance of the rings (the angle between them is 10.97(1) $^o$) is 3.18 Å while the offset of the centroids is 2.03 Å. A packing diagram showing all the interactions described above is presented in Fig. 21.

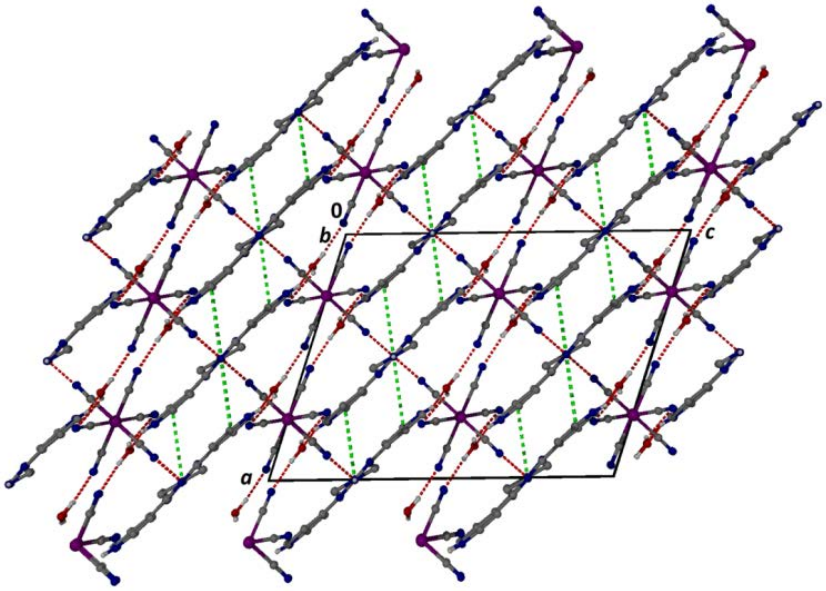


**Figure 21**. A packing diagram of **8** showing H-bonds and stacking interactions with red and green dashed bonds respectively.

**4. Concluding Remarks**

We have successfully synthesized eight new charge assisted supramolecular frameworks by employing the simple molecular building unit $[Fe(CN)_6]^{4-}$ or $[Fe(CN)_6]^{3-}$ as acceptor and protonated nitrogen heterocycles as donors. In general, we have combined the exotopic H-bonding ability of the cyanide ligand with information-poor donors such as single N-H donors. This approach reduces the possibility of control over the crystal structure but it offers greater opportunities in terms of structural and compositional diversity.

While all compounds are new, compounds **5** – **8** are unique in terms of the cation used as donor in cyanometallate supramolecular chemistry. The compounds can be separated in groups depending on some of their characteristics. a) The topological net formed, exists with minor changes, after the removal of the organic cation: Compounds: **3**, **4**, **7**; they increase the number of hexacyanoferrate / protonated N-heterocycle / oxonium systems to 6. The other examples include pyridinium and 2,2'-pyridylpyridinium [22], and $bpeH_2^{2+}$ [12] b) Expansion of the cations connectivity via complex formation with water molecules: Compounds: **5**, **7**, **8**. To our surprise, there are only 11 examples in Cambridge Structural Database [30] containing cyanometallates interacting with supramolecules formed by water and a nitrogen heterocycle. c) Formation of hydrocyanoferrates: Compounds **3**, **7**. The appearance of hydrocyanoferrates is scarce in the literature and in the presence of protonated nitrogen heterocycles only two examples exist. [22] There are three more such anions in crystal lattices with organic non-protonated cations. [31, 32]

At this point we can say that a few factors that govern the resulting solid state formulations between cyanoferrates and protonated nitrogen heterocycles are emerging from the present study. i) In all cases were the planar cations maintain their planarity (**1**, **4**, **7**, **8**) they are parallel to each other in the crystal, forming occasionally stacking interactions. ii) In general, when the ratio between the anion and cation charges is integer (**1**, **6**, **8**) the formulations are simpler and the topologies of the resulting networks are less distorted. iii) The size (**3**, **4**, **7**) and shape (**5**) of the organic cations appear to play important role. Lengthy cations such as $bpeH_2^{2+}$ lead easily to incorporation of hydroniums in the solid formulation. iv) When the organic cations are less than those needed to balance the charge of the anion, hydroniums are formed which eventually participate in the network formation. The organic cations are accommodated in cavities formed in the network. v) The presence of aliphatic

ammonium groups, due to their ability to form more H-bonds as donors than the pyridinium groups, reduces the necessity for oxoniums or for supramolecules that that contain water molecules to stabilize a structure (compare the structure of **6** with the other compounds).

Certainly, more work is essential to shed more light on the factors described above and discover new ones.

**Appendix A. Supplementary Data**

CCDC 1834367-1834374 contain the supplementary crystallographic data for compounds **1** – **8**. These data can be obtained free of charge from The Cambridge Crystallographic Data Centre via www.ccdc.cam.ac.uk/data_request/cif. Supplementary data associated with this article can be found, in the online version, at http://dx.doi.org/_____.

**References**

1. G.R. Desiraju, *Crystal Engineering: The Design of Organic Solid,* Elsevier, Amsterdam, 1989.

2. G.R. Desiraju, J.J. Vittal, A. Ramanan, *Crystal Engineering: A Text Book,* IISc Press and World Scientific, Bangalore, 2011.

3. See for example: a) L. Brammer, J. K. Swearingen, E. A. Bruton, P. Sherwood, Proc. Natl. Acad. Sci. U. S. A. 99 (2002) 4956. b) S. Ferlay, M. W. Hosseini, Chem. Commun., 2004, 788. c) M. Felloni, P. Hubberstey, C. Wilson, M. Schröder, CrystEngComm 6 (2004) 87. d) P. C. Crawford, A. L. Gillon, J. Green, A. G. Orpen, T. J. Podesta, S. V. Pritchard, CrystEngComm 6 (2004) 419.

4. See for example: a) C. B. Aakeroy, K. Beffert, J. Desper, E. Elisabeth, Cryst. Growth Des. 34 (2003) 837. b) D. Braga, L. Maini, M. Polito, E. Tagliavini, F. Grepioni, Coord. Chem. Rev., 246 (2003) 53.

5. G. R. Desiraju, Angew. Chem. Int. Ed. Engl. 34 (1995) 2311.

6. a) S.Mann, Nature (London), 365 (1993) 499. b) A. Jouaiti, M. W. Hosseini, N. Kyritsakas, Chem. Commun. (2003) 472.

7. J.C. Curtis, B.P. Sullivan, T.J. Meyer, Inorg. Chem. 19 (1980) 3833.

8. a) M. Verdaguer, A. Bleuzen, V. Marvaud, J. Vaissermann, M. Seuleiman, C. Desplanches, A. Scuiller, C. Train, R. Garde, G. Galley, C. Lomenech, I. Rosenman, P. Veillet, C. Cartier, F. Villain, Coord. Chem. Rev. 190–192 (1999) 1023. b) M. Ohba, H. Okawa. Coord. Chem. Rev., 198 (2000) 313.

9. K. R. Dunbar, R. A. Heintz, Prog. Inorg. Chem. 45 (1997) 283.

10. H.Eshtiagh-Hosseini, M.Mirzaei, M.Biabani, Vito Lippolis, M.Chahkandi, C.Bazzicalupi, CrystEngComm 15 (2013) 6752.

11. C. Shi, X. Zhang, Y. Cai, Y.-F. Yao, W. Zhang, Angew.Chem.,Int.Ed. 54 (2015) 6206.

12. A.Hazra, G. Kargal, T.K.Maji, Cryst. Growth Des., 13 (2013) 4824.

13. A.Hazra, P.Kanoo, S.Mohapatra, G.Mostafa, T.K.Maji, CrystEngComm 12 (2010) 2775.

14. I. A. Baburin, V. A. Blatov, L. Carlucci, G. Ciani and D. M. Proserpio, Cryst. Growth Des. 8 (2008) 519.

15. F.H. Allen, Acta Cryst. B58 (2002) 380–388.

16. M.C. Burla, R. Caliandro, B. Carrozzini, G. L. Cascarano, C. Cuocci, C. Giacovazzo, M. Mallamo, A. Mazzone, G. Polidori, J. Appl. Cryst. 48 (2015) 306.

17. G.M. Sheldrick, Acta Cryst. C71 (2015) 3.

18. C. B. Hübschle, G. M. Sheldrick, B. Dittrich, J. Appl. Cryst. 44 (2011) 1281.

19. M. Nardelli, J. Appl. Cryst. 32 (1999) 563.

20. V. A. Blatov, A. P. Shevchenko, D. M. Proserpio, Cryst. Growth Des., 14 (2014) 3576.

21. N.W.Alcock, A.Samotus, J.Szklarzewicz, J.Chem.Soc.,Dalton Trans. (1993), 885

22. S. I. Gorelsky, A. B. Ilyukhin, P. V. Kholin, V. Yu. Kotov, B. V. Lokshin, N. V. Sapoletova, Inorg. Chim. Acta 360 (2007) 2573.

23. M. Pierrot, R. Kern, R. Weis, Acta Cryst. 20 (1966) 425.

24. R. Haser, C. E. De Broin, M. Pierrot, Acta Cryst. B28 (1972) 2530.

25. X.-Z. Yang, A.-Y. Hu, A.-H. Yuan, Acta Crystallogr., E69 (2013) m132.

26. S.A. Adonin, M.E. Rakhmanova, D. G. Samsonenko, M. N. Sokolov, V. P. Fedin, Polyhedron 98 (2015) 1.

27. H. M. Titi, I. Goldberg, CrystEngComm 12 (2010) 3914.

28. C. J. Burchell, C. Glidewell, A. J.Lough, G. Ferguson, Acta Crystallogr.,B57 (2001) 201.

29. S. R. Batten, S. M. Neville, D. R. Turner, Coordination Polymers: Design, Analysis and Application, 2009, RSC Publishing, Cambridge, UK.

30. C. R. Groom, I. J. Bruno, M. P. Lightfoot, S. C. Ward, Acta Crystallogr. B72 (2016) 171. CSD codes: Fe, ZANPIP, DODDUI; Mo, MEXLUY; W, BOFROE, GOWZOH, MUBXIR, PECMOZ; Pt, EXONAH, EXONEL, SAKNEY; Nb, XETYAY.

31. M. N. Zhidkova, V. K. Laurinavichyute, Y. V. Nelyubina, V. Yu. Kotov, J. Sol. Chem. 44 (2015) 1240.

32. M. N. Zhidkova, K. E. Aysina, V. Yu. Kotov, V. K. Ivanov, Y. V. Nelyubina, I. V. Ananyev, V. K. Laurinavichyute, Electrochim. Acta 219 (2016) 673.